

AD-A039 758

SOUTHWEST RESEARCH INST SAN ANTONIO TEX ARMY FUELS A--ETC F/G 21/4
RHEOLOGY STUDY OF ANTIMIST FUELS.(U)
JAN 77 R J MANNHEIMER

UNCLASSIFIED

FAA-RD-77-10

DOT-FA75WAI-571
NL

1 OF 1
ADA039 758



Report No. FAA-RD-77-10

12

AD A 039758

RHEOLOGY STUDY OF ANTIMIST FUELS

R. J. Mannheimer



JANUARY 1977

FINAL REPORT

Document is available to the U.S. public through
the National Technical Information Service,
Springfield, Virginia 22161.



Prepared for

U.S. DEPARTMENT OF TRANSPORTATION
FEDERAL AVIATION ADMINISTRATION
Systems Research & Development Service
Washington, D.C. 20590

AD NO. 1
DDC FILE COPY

NOTICE

This document is disseminated under the sponsorship of the Department of Transportation in the interest of information exchange. The United States Government assumes no liability for its contents or use thereof.

The contents of this report reflect the views of the U. S. Army Fuels and Lubricants Research Laboratory which is responsible for the facts and the accuracy of the data presented herein. The contents do not necessarily reflect the official views or policy of the Department of Transportation. This report does not constitute a standard, specification or regulation.

Technical Report Documentation Page

1. Report No. 18 FAA-RD-77-10	2. Government Accession No.	3. Recipient's Catalog No.	
4. Title and Subtitle 6 RHEOLOGY STUDY OF ANTIMIST FUELS	5. Report Date 11 January 1977	6. Performing Organization Code	
7. Author(s) 10 R. J. Mannheimer	8. Performing Organization Report No. 12 54 P.	9. Performing Organization Name and Address U.S. Army Fuels & Lubricants Research Laboratory Southwest Research Institute P.O. Box 28510 San Antonio, Texas 78284	
10. Work Unit No. (TRAIS) 181-520	11. Contract or Grant No. 15 DOT-FA75WAI-571	12. Sponsoring Agency Name and Address U.S. Department of Transportation Federal Aviation Administration Systems Research and Development Service Washington, D.C.	
13. Type of Report and Period Covered 9 Final Report 1 Jul 1975 - Dec 1976	14. Sponsoring Agency Code ARD-520	15. Supplementary Notes	
16. Abstract Two different rheological phenomena have been studied that may relate to the mechanisms by which high molecular weight polymers inhibit misting. The first of these is a shear thickening or antithixotropic phenomenon in which the liquid fuel develops a shear induced structure above a critical shear stress. The second phenomenon involves the sudden increase in resistance to flow in porous media that certain polymer solutions exhibit when the flow rate is above a critical value. This effect is quite different from the first in that the former can be induced by shear while the latter requires elongation. While it is difficult to interpret these phenomena directly in terms of shear and elongational viscosities, it appears possible that the critical shear stress and the critical flow rate may be useful criteria for characterizing the condition of the antimist additive. The theoretical significance of the critical flow rate in porous media has been discussed in terms of a fluid relaxation time which in turn may be related to the polymer molecular weight. A relationship between the critical flow rate and the intrinsic viscosity is presented that explains why the former is more sensitive to polymer degradation.			
17. Key Words Rheology Viscoelasticity Polymer Solutions		18. Distribution Statement Document is available to the public through the National Technical Information Service, Springfield, Virginia 22151	
19. Security Classif. (of this report) Unclassified	20. Security Classif. (of this page) Unclassified	21. No. of Pages 50	22. Price

METRIC CONVERSION FACTORS

Approximate Conversions to Metric Measures

Symbol When You Know Multiply by To Find Symbol

LENGTH

inches
feet
yards
miles

Centimeters
meters
kilometers

cm
m
km

AREA

square inches
square feet
square yards
square miles
acres

square centimeters
square meters
square kilometers
hectares

cm²
m²
km²
ha

MASS (weight)

ounces
pounds
short tons
(2000 lb)

grams
kilograms
tonnes

g
kg
t

VOLUME

teaspoons
tablespoons
fluid ounces
cups
pints
quarts
gallons
cubic feet
cubic yards

milliliters
milliliters
milliliters
liters
liters
liters
liters
cubic meters
cubic meters

ml
ml
ml
l
l
l
l
m³
m³

TEMPERATURE (exact)

Fahrenheit
temperature

Celsius
temperature

°F

Approximate Conversions from Metric Measures

When You Know Multiply by To Find Symbol

LENGTH

millimeters
centimeters
meters
kilometers

inches
inches
feet
yards
miles

in
in
ft
yd
mi

AREA

square centimeters
square meters
square kilometers
hectares (10,000 m²)

square inches
square yards
square miles
acres

in²
yd²
mi²

MASS (weight)

grams
kilograms
tonnes (1000 kg)

ounces
pounds
short tons

oz
lb

VOLUME

milliliters
liters
liters
liters
cubic meters
cubic meters

fluid ounces
pints
quarts
gallons
cubic feet
cubic yards

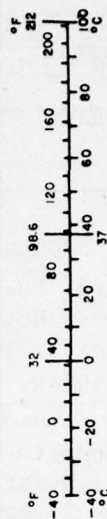
fl oz
pt
qt
gal
ft³
yd³

TEMPERATURE (exact)

Celsius
temperature

Fahrenheit
temperature

°C




*1 in 2 3/4 inch. For other exact conversions and more detailed tables, see NBS Misc. Publ. 286, Units of Weights and Measures, Price \$2.25, SD Catalog No. C13.10.286.

TABLE OF CONTENTS

	<u>Page</u>
LIST OF FIGURES	vi
LIST OF TABLES	vii
Preface	1
Summary	2
Objectives	3
Approach	3
Results	3
A. Shear Viscosity	3
1. AM-1	3
2. XD-8132.01	7
3. FM-9	12
B. Intrinsic Viscosity	18
C. Viscoelasticity	22
1. Different AM-1 Samples	24
2. Effect of Blending	27
3. Flow and Ultrasonic Degradation	31
4. Theoretical Significance of the Critical Flow Rate	35
D. Physical Properties of Antimist Fuels (0.30% AM-1 in Jet-A) Used in Fuel Spillage/Air Shear Tests	37
1. Comparison of AFLRL and NAPTC AM-1 Samples Blended at NWC	37
Conclusions and Recommendations	39
LIST OF REFERENCES	43

43

NTIS DOC UNANNOUNCED JUSTIFICATION.....	White Section <input checked="" type="checkbox"/> Buff Section <input type="checkbox"/> <input type="checkbox"/>
BY.....	
DISTRIBUTION/AVAILABILITY CODES	
Dist.	AVAIL. AND/OR SPECIAL
A	

LIST OF FIGURES

<u>FIGURE No.</u>		<u>PAGE</u>
1	Sketch of Capillary Tube Apparatus for Measuring Shear Viscosity	4
2	Flow of Antimist Fuel (0.21 wt% AM-1 in JP-8) in A Capillary Tube at Low to Moderate Shear Rates	5
3	Flow of Antimist Fuel (0.21 wt% AM-1 in JP-8) in Capillary Tubes at High to Very High Shear Rates	8
4	Characteristic Shear Thinning of Antimist Fuel (0.21 wt% AM-1 in JP-8)	9
5	Flow of Antimist Fuel (0.7 wt% XD-8132.01 in Jet-A) in a Capillary Tube	10
6	Flow of Antimist Fuel (0.7 wt% XD-8132.01 in DF-2) in a Capillary Tube	11
7	Flow of Antimist Fuel (0.287 wt% FM-9 in Avtur) in a Capillary Tube	13
8	Flow of Antimist Fuel (0.287 wt% FM-9 in Avtur) in a Capillary Tube	14
9	Time Dependent Shear Thickening of Antimist Fuel (0.287 wt% FM-9 in Avtur) in a Capillary Tube	15
10	Shear Thickening of Antimist Fuel (0.287 wt% FM-9 in Avtur) with a Cone (1°) and Plate Viscometer	16
11	Reduced or Inherent Viscosity of AM-1 (AFLRL) in JP-8 by Two Different Methods	19
12	Dimensionless Reduced or Inherent Viscosity of AM-1 in JP-8 (Std. Tube)	21
13	Dimensionless Reduced or Inherent Viscosity of FM-9 in Avtur by Two Different Methods	23
14	Determination of Onset of Anomalous (Viscoelastic) Resistance of Dilute AM-1 Solution to Flow in Porous Media	25
15	Anomalous (Viscoelastic) Resistance of Antimist Fuels Made With AM-1 From Different Sources	26
16	Effect of Blending Technique on Anomalous (Viscoelastic) Resistance of Antimist Fuels	28
17	Effect of Concentration on Mist-Flash-Back of Antimist Fuels (AM-1 in JP-8) from AFLRL and NAPTC	30
18	Ultrasonic Device for Degrading Antimist Fuels	32
19	Effect of Flow and Ultrasonic Degradation on the Anomalous (Viscoelastic) Resistance of Antimist Fuels (0.025 wt% AM-1 in JP-8) to Flow in Porous Media	33
20	Correlation of Critical Flow Rate in Porous Media and Intrinsic Viscosity* For Partially Degraded Antimist Fuels (0.025 wt% AM-1 in JP-8)	38
21	Intrinsic Viscosities of Antimist Fuels Used in Fuel Spillage/Air Shear Tests at NWC	40
22	Anomalous (Viscoelastic) Resistance to Flow in Porous Media of Antimist Fuels (0.30% Diluted to 0.025% AM-1 in Jet-A) Used in Fuel Spillage/Air Shear Tests at NWC	41

LIST OF TABLES

<u>TABLE No.</u>		<u>Page</u>
1	Typical Physical Properties of JP-8, Jet-A and Avtur Aviation Fuels	6
2	Critical Shear Stress at Onset of Shear Thickening (0.287 wt% FM-9 in Avtur at 25-26°C)	17
3	Effect of Flow and Ultrasonic Degradation on Rheological Properties of Antimist Fuel (0.20 wt% in JP-8)	34

Preface

This report was prepared by the U.S. Army Fuels and Lubricants Research Laboratory (AFLRL) at Southwest Research Institute (SwRI), San Antonio, Texas, for the Federal Aviation Administration. The work was performed from July 1, 1975 to December 31, 1976 under the management of Mr. T.G. Horeff, Aircraft Design Criteria Branch, Aircraft Safety and Noise Abatement Division, Systems Research and Development Service, Federal Aviation Administration, Washington, D.C.

Mr. B.R. Wright of SwRI designed the apparatus used in the ultrasonic degradation studies and Messrs. J.L. Jungman and G.W. Kuykendall of SwRI performed the rheological measurements.

PRECEDING PAGE BLANK-NOT FILMED

Summary

Antimist fuels, made with either the Dow (XD-8132.01) or ICI (FM-9) additives, have been found to form a gel-like solid above a critical shear stress. While it is difficult to interpret these measurements directly in terms of a shear viscosity, it appears possible that the critical shear stress can be used to distinguish between the relative effectiveness or degree of degradation of shear thickening additives.

Antimist fuels made with the Conoco (AM-1) additive do not shear thicken but have been found to exhibit a very high resistance to flow in porous media that is a measure of their viscoelasticity. By working with very dilute solutions, it has been shown that while the resistance can initially be predicted by the shear viscosity, it suddenly becomes very large when the flow rate exceeds a critical value. Although these two phenomena appear to be similar, they are actually quite different in that the former can be induced by shear while the latter requires elongation. These experimental results are again difficult to interpret directly in terms of an elongational viscosity, however it has been shown that the critical flow rate can readily discriminate between antimist fuels made with additives from different batches and with additives that have been partially degraded by flow or ultrasonic energy.

The intrinsic viscosity has also been found useful in characterizing antimist fuels and has the important advantage over the shear viscosity, in that it is independent of the polymer concentration and is only slightly dependent on the temperature and the shear rate. On the other hand, if the intrinsic viscosity is known, it has been shown that the dimensionless intrinsic viscosity can be used to estimate the polymer concentration. The important point is that the dimensionless intrinsic viscosity can be measured in the field while the antimist fuel is being blended.

The theoretical significance of the critical flow rate in porous media has been discussed in terms of a fluid relaxation time which in turn can be related to the polymer molecular weight. Furthermore, a theoretical basis for the correlation between the critical flow rate and intrinsic viscosity of partially degraded viscoelastic additives has been given that explains why the critical flow rate is more sensitive to degradation.

While preliminary results of fuel-spillage/air-shear tests indicate that both the critical flow rate and intrinsic viscosity are important factors in determining the relative effectiveness of viscoelastic additives, additional field and full-scale fire-safety tests are needed in order to determine the minimum values of these quantities that are needed for a fire-safety fuel specification.

Objectives

The primary objectives of this program were to develop methods of measuring the rheological properties of antimist fuels and to establish the relationships between these properties and fuel fire safety that are related to impact-survivable aircraft crashes.

Approach

Since dilatancy (shear thickening) and viscoelasticity (elongational viscosity) were thought to be important in preventing mist formation, these are the primary rheological properties that were studied; however other factors, such as intrinsic viscosity, that provide basic information pertaining to the size of polymer molecules in solution, were also considered. While it was originally intended to thoroughly investigate several candidate additives,* the supply of XD-8132.01 (Dow) was curtailed early in the program, and FM-9 (ICI) was not available until late in the program; consequently, our primary effort has been with AM-1 (Conoco). The shear viscosity of antimist fuels was measured with capillary and rotational viscometers, and viscoelasticity was determined from the onset of anomalous resistance to flow in porous media.

Results

A. Shear Viscosity

While a capillary viscometer is not ideally suited for characterizing rheologically complex fluids, important information concerning the shear viscosity can often be obtained if flow data are expressed in terms of the wall shear stress ($T = R\Delta P/2L$, where R is the capillary radius, ΔP is the pressure drop, and L is the capillary length) and wall shear rate ($D = 4Q/\pi R^3$, where Q is the volumetric flow rate). This latter quantity is the magnitude of the shear rate for a Newtonian liquid, however it is often a good first approximation even for non-Newtonian fluids. In these experiments flow data were obtained by applying a positive pressure to a fluid reservoir and measuring the mass flow rate by collecting and weighing a sample of fluid over a measured time interval (usually one minute). For very low pressures, the gas/liquid interface in the fluid reservoir could be adjusted to provide a fluid head relative to the centerline of the capillary tube which was held in a horizontal position (see Figure 1). Other than the room temperature being approximately constant (77-80°F), no special bath was provided to control the fuel temperature.

1. AM-1

The results presented in Figure 2 are for an antimist fuel consisting of 0.21% AM-1** in JP-8.*** Over the range of shear rates from 200 to 2000 sec^{-1} , this antimist fuel exhibits a slightly non-linear flow curve that is typical for most dilute polymer solutions, i.e., the

*These are proprietary polymers that generally have a molecular weight in excess of one million.

**wt% was determined by steam-jet gum (ASTM D-381).

***Typical physical properties of JP-8, Jet-A and Avtur are summarized in Table 1.

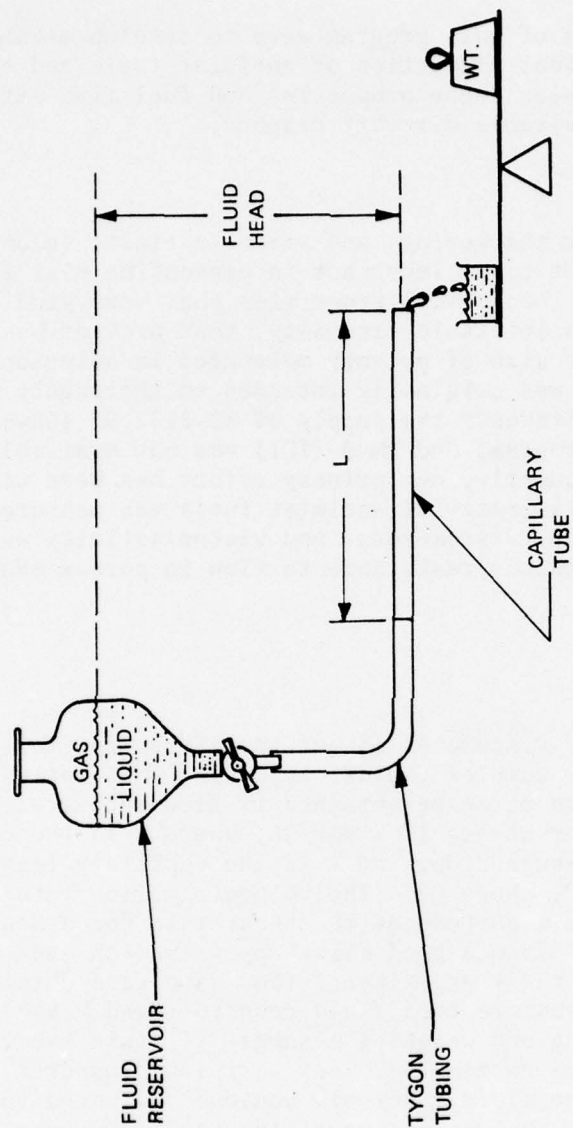


FIGURE 1. SKETCH OF CAPILLARY TUBE APPARATUS FOR MEASURING SHEAR VISCOSITY.

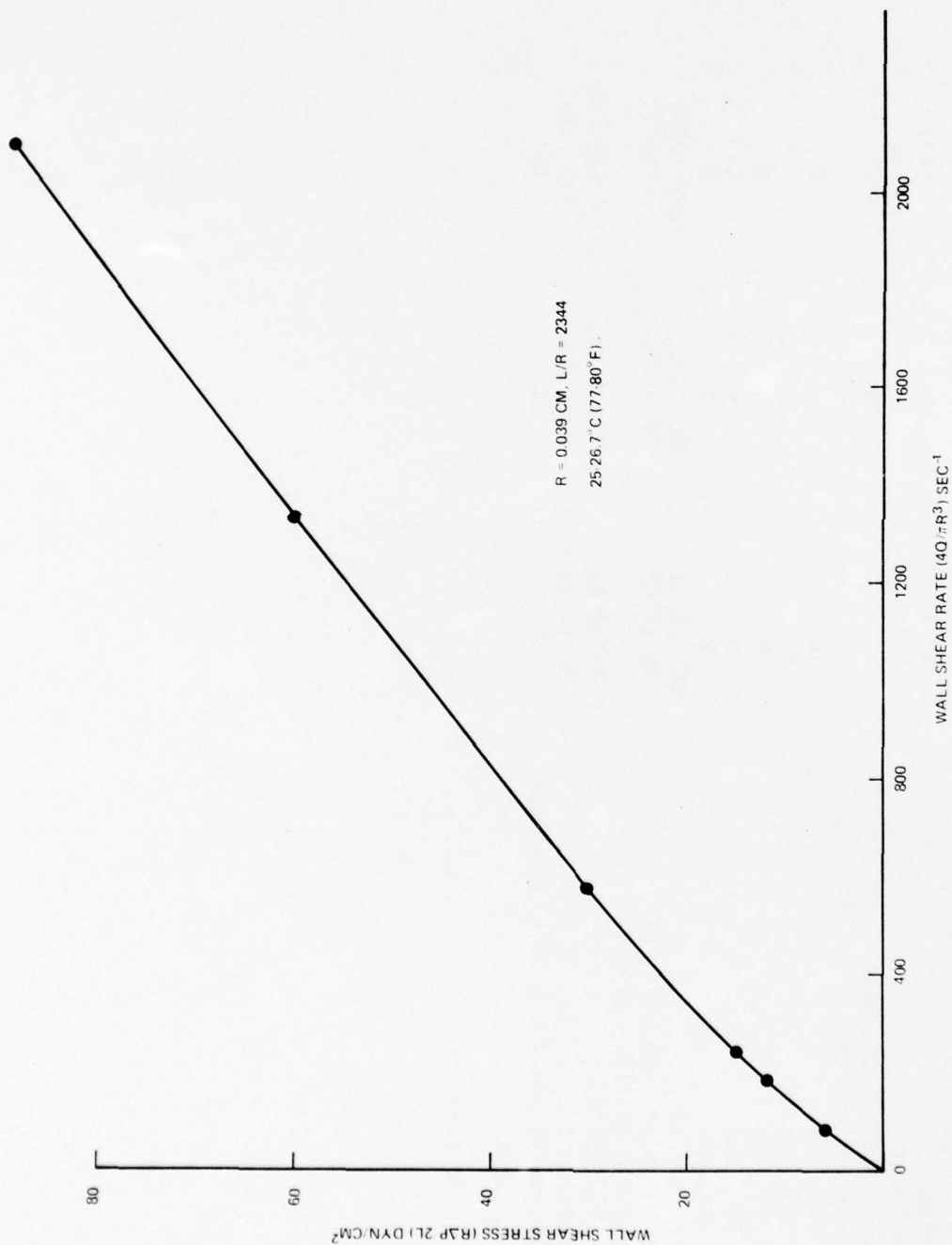


FIGURE 2. FLOW OF ANTIMIST FUEL (0.21 wt% AM-1 in JP-8) IN A CAPILLARY TUBE AT LOW TO MODERATE SHEAR RATES.

TABLE 1. TYPICAL PHYSICAL PROPERTIES OF JP-8,
JET-A AND AVTUR AVIATION FUELS

Specification	MIL-T-83133	ASTM 1655	D Eng. RD 2494
Product	JP-8	Jet-A	Avtur
Nato Code	F-34	-----	F-35
Aromatics, % vol, max	25	22	25
Distillation Temp., °C (°F):			
IBP	R*	-----	R
10%, max	205	205	-----
20%, max	R	-----	R
50%, max	R	R	R
90%, max	R	R	R
FBP	300 (572)	300 (572)	288 (550)
Flash point, min, °C (°F)	38 (100)	38 (100)	38 (100)
Specific gravity, 15°C (59°F)/ 15°C (59°F)	0.775-0.840	0.775-0.840	0.775-0.830
Freezing point, max, °C (°F)	-50 (-58)	-40 (-40)	-50 (-58)
Viscosity, -34.4°C (-30°F) max, cSt	15	15	15

* - R denotes report.

shear resistance decreases with shear rate. At very high shear rates of 20,000 to 200,000 sec⁻¹ (Figure 3) the flow curve appears to be that of a Newtonian or shear independent fluid; however this is due in part to the scale and the fact that we are approaching the limiting value of the high shear rate viscosity. Because of the small degree of non-linearity, the correction to D to obtain the true shear rate at the tube wall can be neglected, i.e.,

$$|\dot{\gamma}|_R = \frac{T}{4} \left(\frac{dD}{dT} + \frac{3D}{T} \right) \approx D, \text{ when } \frac{dD}{dT} \approx \frac{D}{T} \quad (1)$$

so that the shear viscosity can be approximated by:

$$\eta \approx \frac{T}{D} \quad (2)$$

The shear viscosity data for AM-1 (0.21 wt% in JP-8) are presented in Figure 4 over four decades of shear rates. The use of the viscosity ratio ($\eta_r = \eta/\eta_0$, where η_0 is the viscosity of the solvent) instead of the absolute viscosity has the advantage that the former is relatively insensitive to temperature. From the results in Figure 4 it is clear that at this concentration, the shear viscosity of AM-1 in JP-8, decreases with shear rate. Consequently, it would appear that the shear viscosity of this antimist fuel is not a significant factor in preventing mist formation; however, we will see later that the shear viscosity of the solvent does influence the relaxation time of the solution which is of primary importance to viscoelastic phenomena.

2. XD-8132.01

Radically different behavior was observed for antimist fuels containing XD-8132.01. For example, the flow data in Figure 5 show that a solution of 0.7wt% XD-8132.01 in Jet-A is essentially Newtonian ($\eta = 9$ cp, $\eta_0 = 1.4$ cp) below a critical shear stress of 100 dyn/cm², actually a very slight amount of shear thinning occurred but it is not evident on this scale. As the stress is increased, there is a sudden and dramatic increase in the shear resistance, indicated by the steepness of the slope of the flow curve, that coincides with the fuel taking on the appearance of a gel-like solid. This type of rheological phenomenon (which is probably due to a flow induced structure resulting from polymer entanglement) is relatively rare, particularly in light of the very large increase in shear viscosity that is produced in a relatively dilute solution with a low viscosity solvent. While data taken at increasing and decreasing pressures did not differ appreciably, it is evident that the transition from the Newtonian or slightly shear thinning regime to the shear thickening regime is not smooth and that some of the data near the critical stress are not equilibrium values. The dotted curve in Figure 5 is an estimate of the expected equilibrium curve and is based on a few preliminary measurements with a cone and plate viscometer in which the critical shear stress was appreciably less than 100 dyn/cm².

The results presented in Figure 6 are for the same additive in a different solvent (diesel fuel). Very similar flow behavior was observed with the exception that the critical stress required to initiate shear thickening was an order of magnitude higher (1000 dyn/cm²

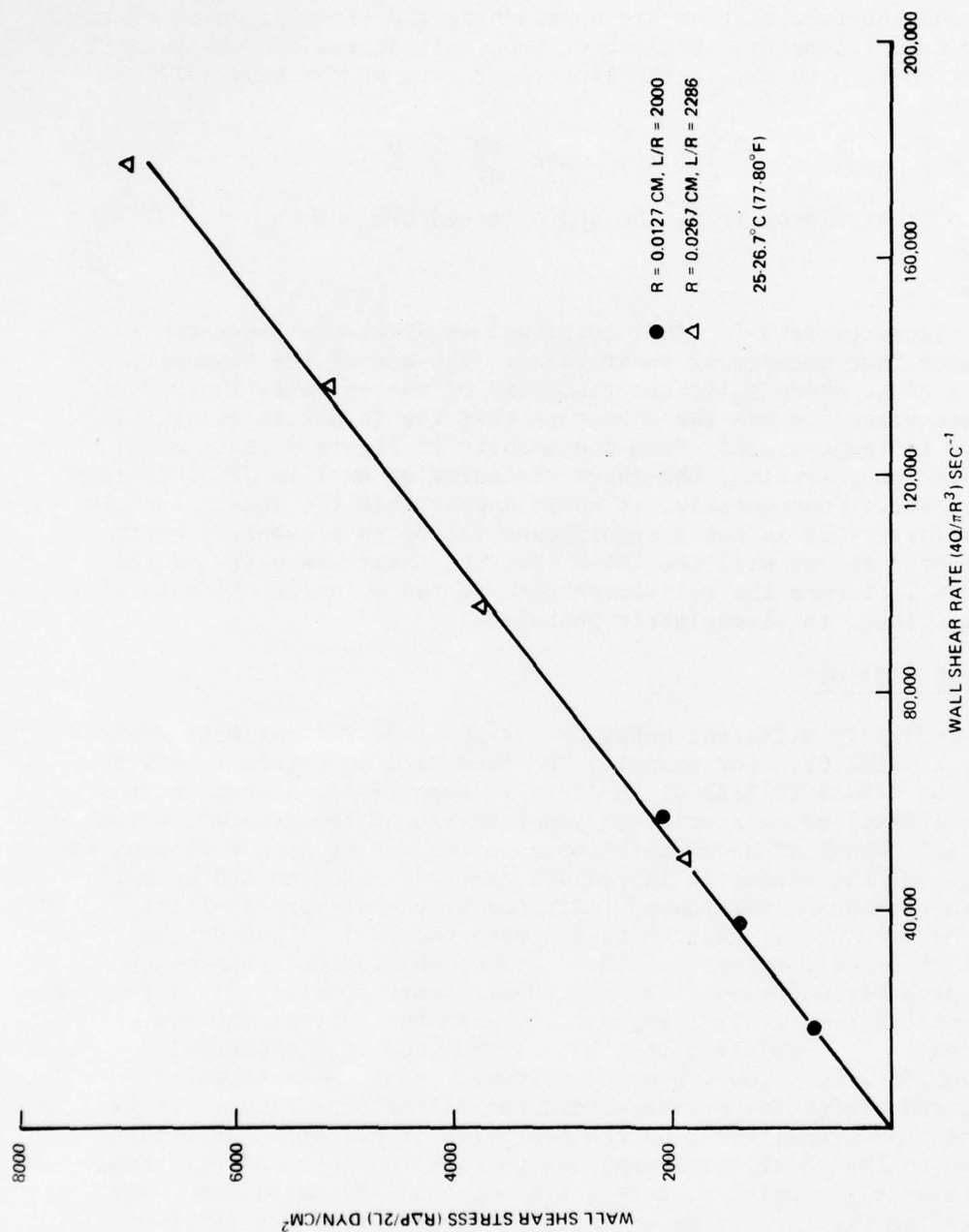


FIGURE 3. FLOW OF ANTIMIST FUEL (0.21 wt% AM-1 in JP-8) IN CAPILLARY TUBES AT HIGH TO VERY HIGH SHEAR RATES.

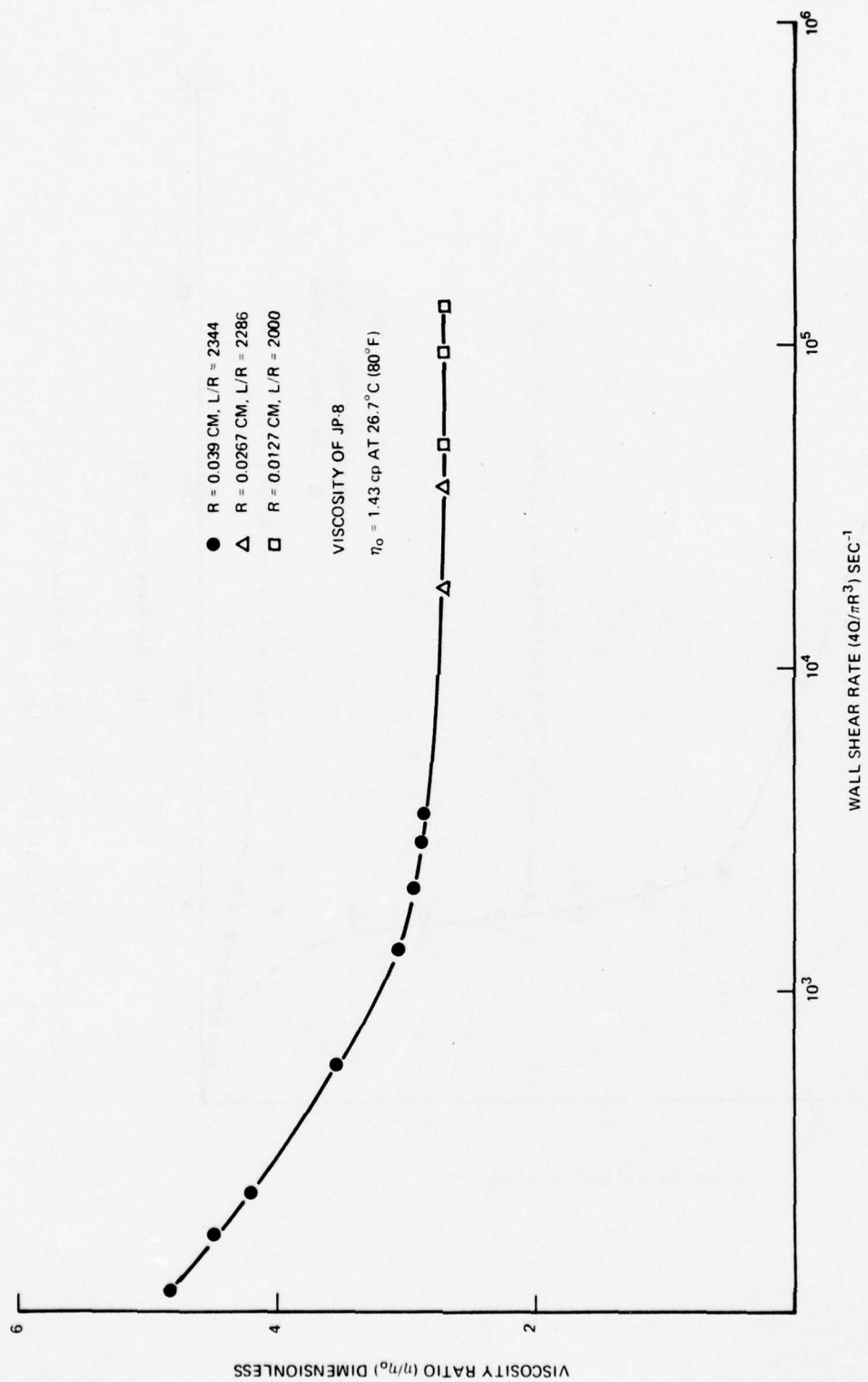


FIGURE 4. CHARACTERISTIC SHEAR THINNING OF ANTIMIST FUEL (0.21 wt% AM-1 in JP-8).

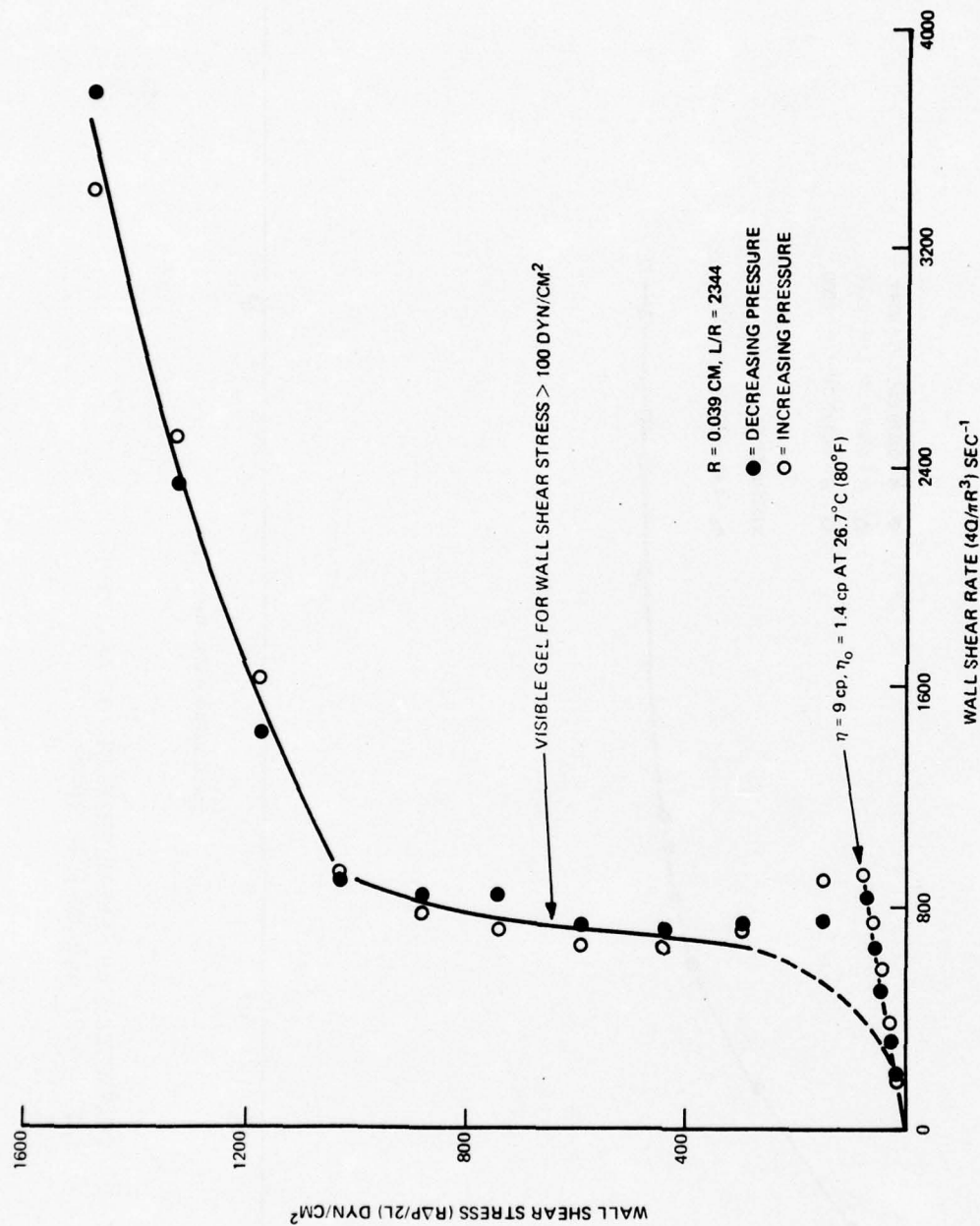


FIGURE 5. FLOW OF ANTIMIST FUEL (0.7 wt% XD-8132.01 in Jet-A) IN A CAPILLARY TUBE.

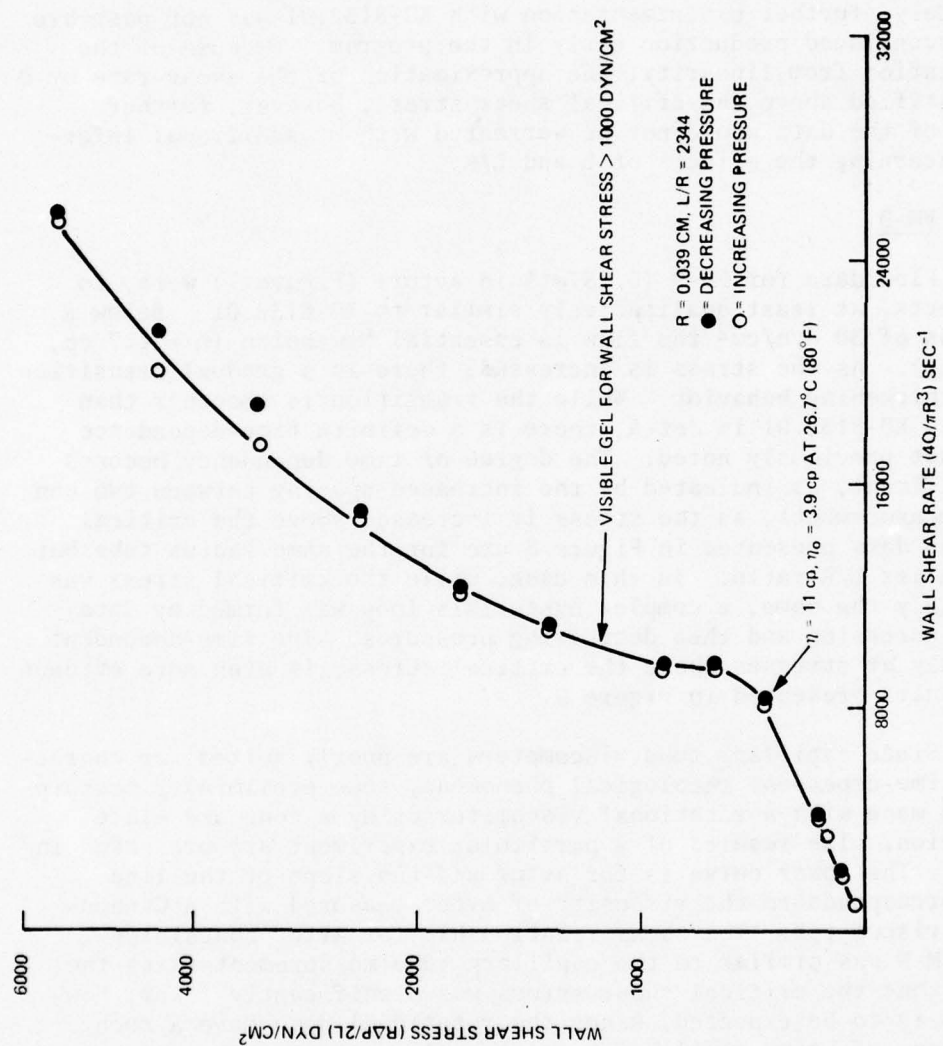


FIGURE 6. FLOW OF ANTIMIST FUEL (0.7 wt% XD-8132.01 in DF-2) IN A CAPILLARY TUBE.

compared to 100 dyn/cm²). Furthermore, the transition from Newtonian to shear thickening was less abrupt. While the reasons for these differences have not been established, it is suspected that they might be related to differences in solvency that would be reflected by different intrinsic viscosities for this additive in Jet-A and diesel fuel. Unfortunately, further experimentation with XD-8132.01 was not possible due to discontinued production early in the program. Because of the large deviation from linearity, the approximation of the shear rate by $\dot{\gamma}$ is not justified above the critical shear stress; however, further reduction of the data would not be warranted without additional information concerning the effects of L and L/R .

3. FM-9

Flow data for FM-9 (0.287wt% in Avtur) (Figure 7) were, in many respects, at least qualitatively similar to XD-8132.01. Below a wall stress of 30 dyn/cm² the flow is essential Newtonian ($\eta = 1.7$ cp, $\eta_0 = 1.0$ cp). As the stress is increased, there is a gradual transition to shear thickening behavior. While the transition is smoother than with 0.7wt% XD-8132.01 in Jet-A, there is a definite time-dependence that was not previously noted. The degree of time dependency becomes more significant, as indicated by the increased spacing between two consecutive measurements, as the stress is increased above the critical value. The data presented in Figure 8 are for the same radius tube but with a smaller L/R ratio. In this case, while the critical stress was approximately the same, a complex hysteresis loop was formed by data taken at increasing and then decreasing pressures. The time-dependent nature, only at stresses above the critical stress, is even more evident in the results presented in Figure 9.

Since capillary tube viscometers are poorly suited for characterizing time-dependent rheological phenomena, some preliminary measurements were made with a rotational viscometer using a cone and plate configuration. The results of a particular experiment are presented in Figure 10. The lower curve is for Avtur and the slope of the line closely corresponds to the viscosity of Avtur measured with a Cannon-Ubbelohde viscometer. The shear relationship for Avtur containing 0.287wt% FM-9 was similar to the capillary tube measurements with the exception that the critical shear stress was significantly lower; however, this is to be expected, since the rotational data have a much better chance of being equilibrium values. A summary of the estimated critical shear stress at the onset of shear thickening is presented in Table 2. While the critical shear stress for the flow experiments are higher than the rotational viscometer measurements, there is also definite evidence of a dependence of the critical shear stress on the viscosity ratio which varied significantly. Since it has recently been learned that FM-9 slowly degrades its antimisting properties when stored in a steel container, it is suspected that some of the experimental difficulties experienced with this additive were a result of this deterioration. In the future, measurements should be made over a short time interval in order to avoid aging effects with the FM-9 additive.

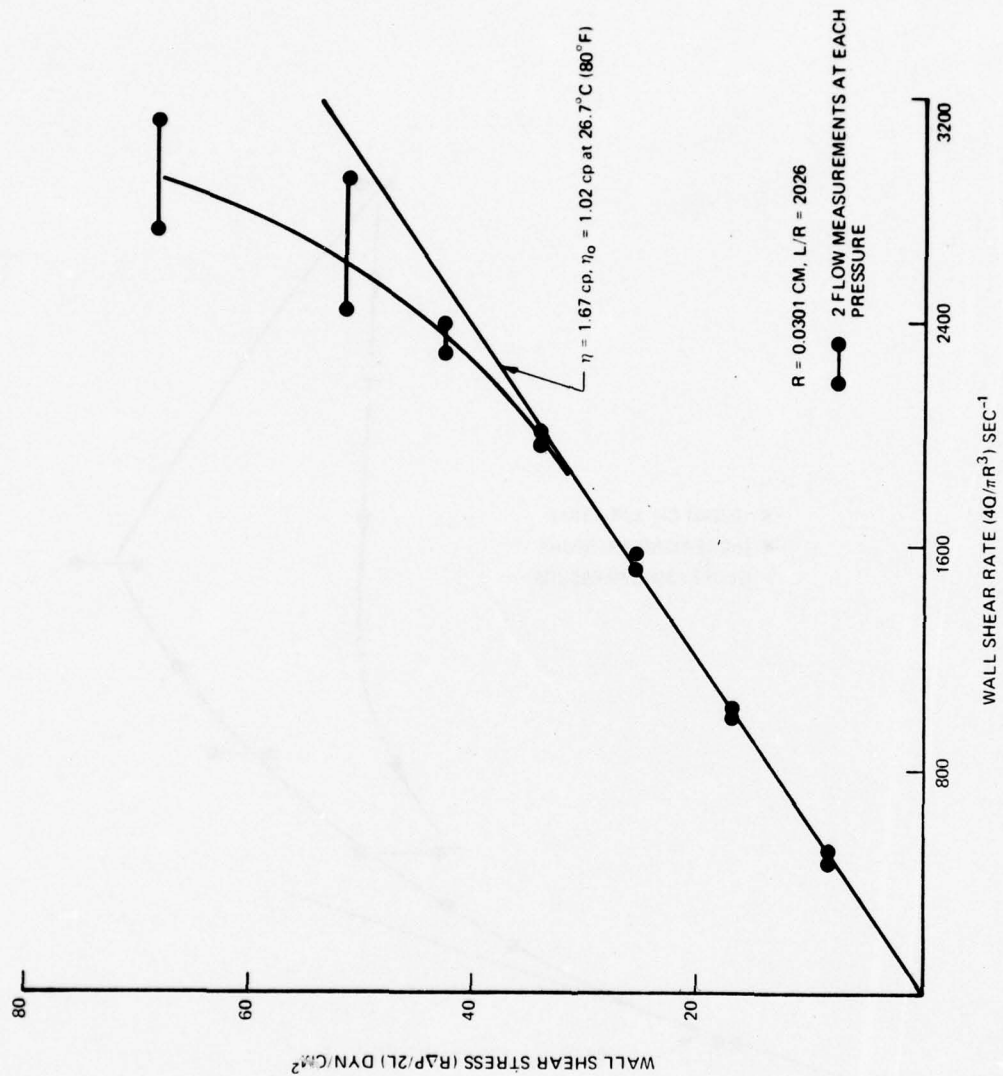


FIGURE 7. FLOW OF ANTIMIST FUEL (0.287 wt% FM-9 in Avtur) IN A CAPILLARY TUBE.

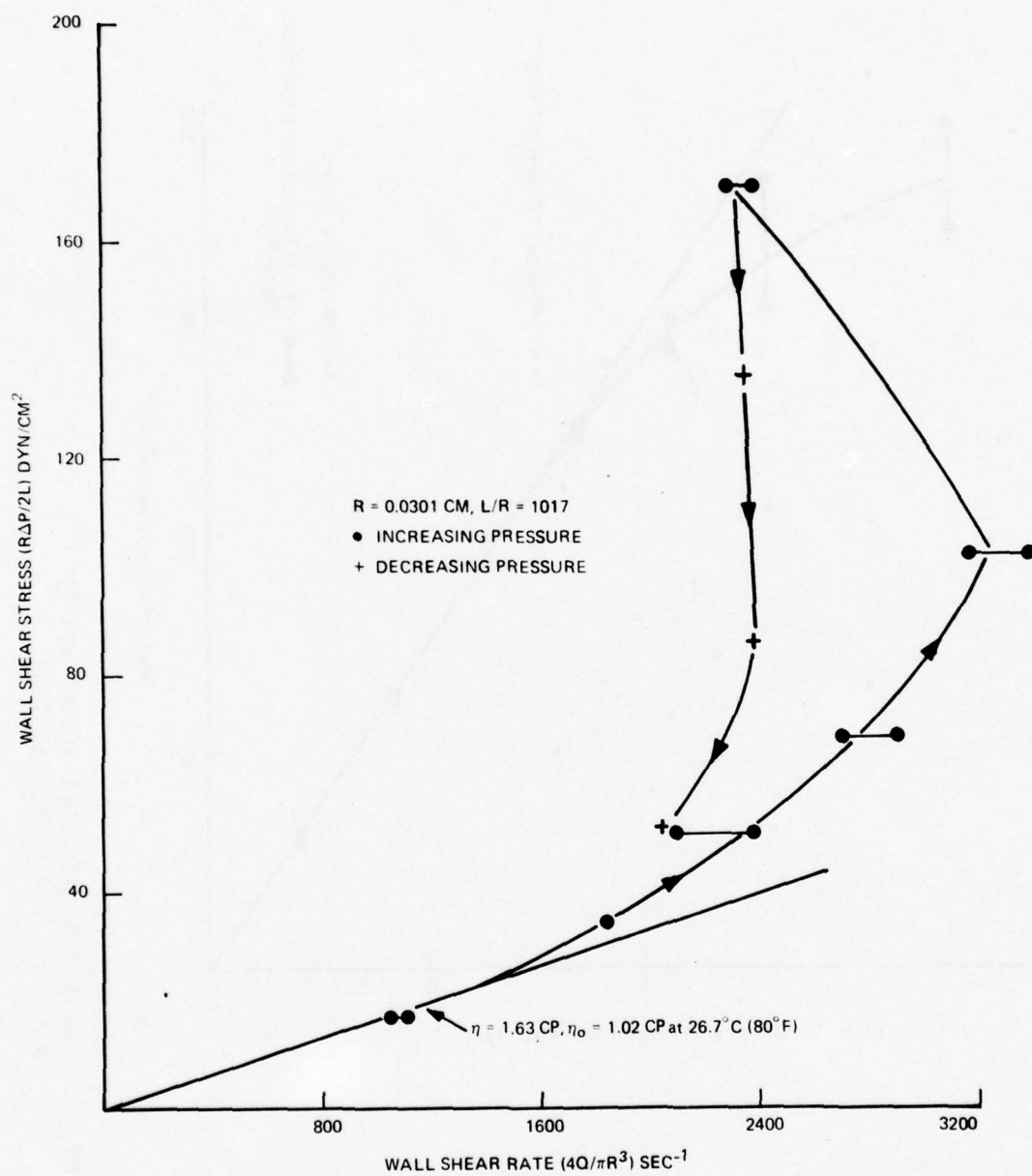


FIGURE 8. FLOW OF ANTIMIST FUEL (0.287 wt% FM-9 in Avtur) IN A CAPILLARY TUBE.

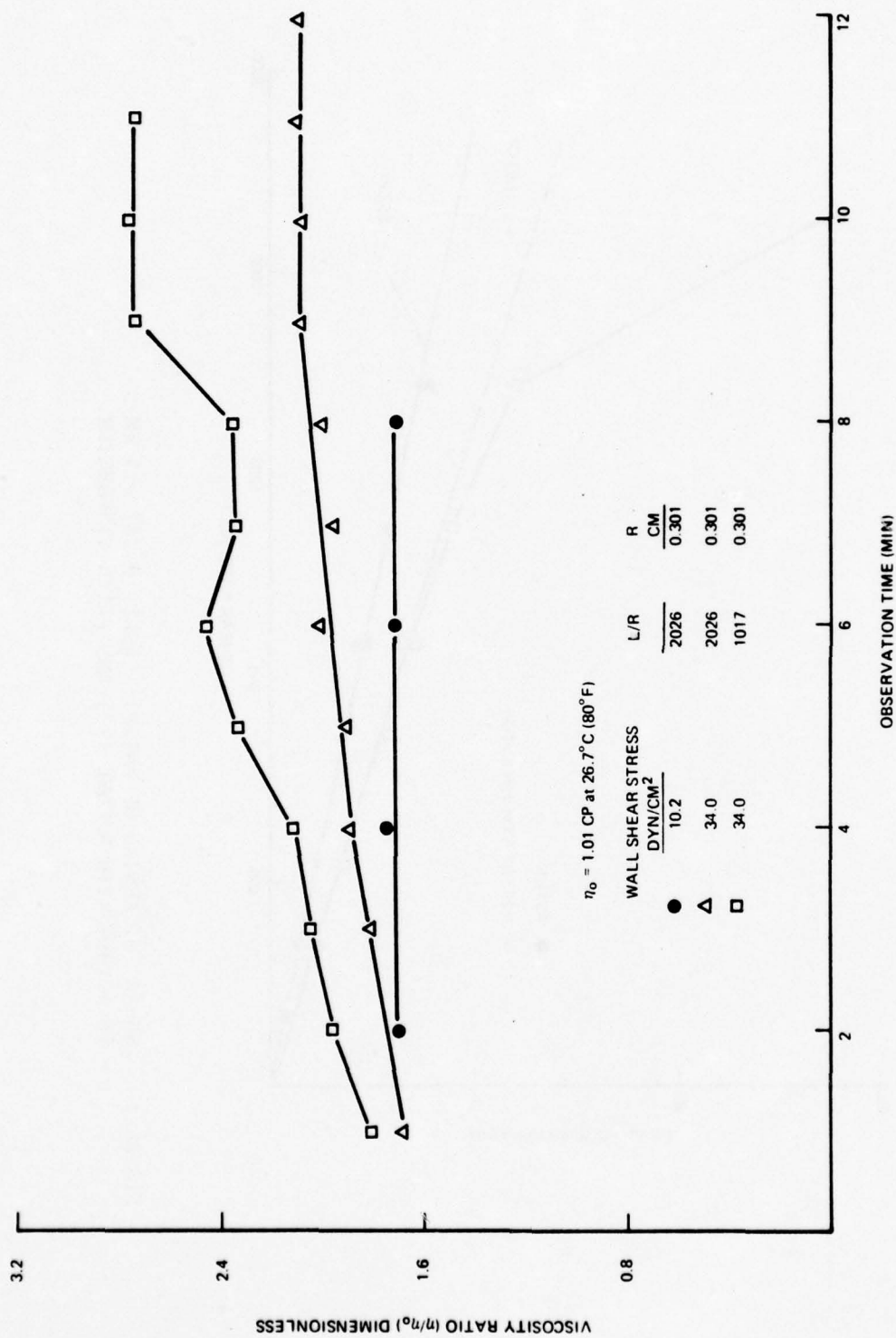


FIGURE 9. TIME DEPENDENT SHEAR THICKENING OF ANTIMIST FUEL (0.287 wt% FM-9 in Avtur) IN A CAPILLARY TUBE.

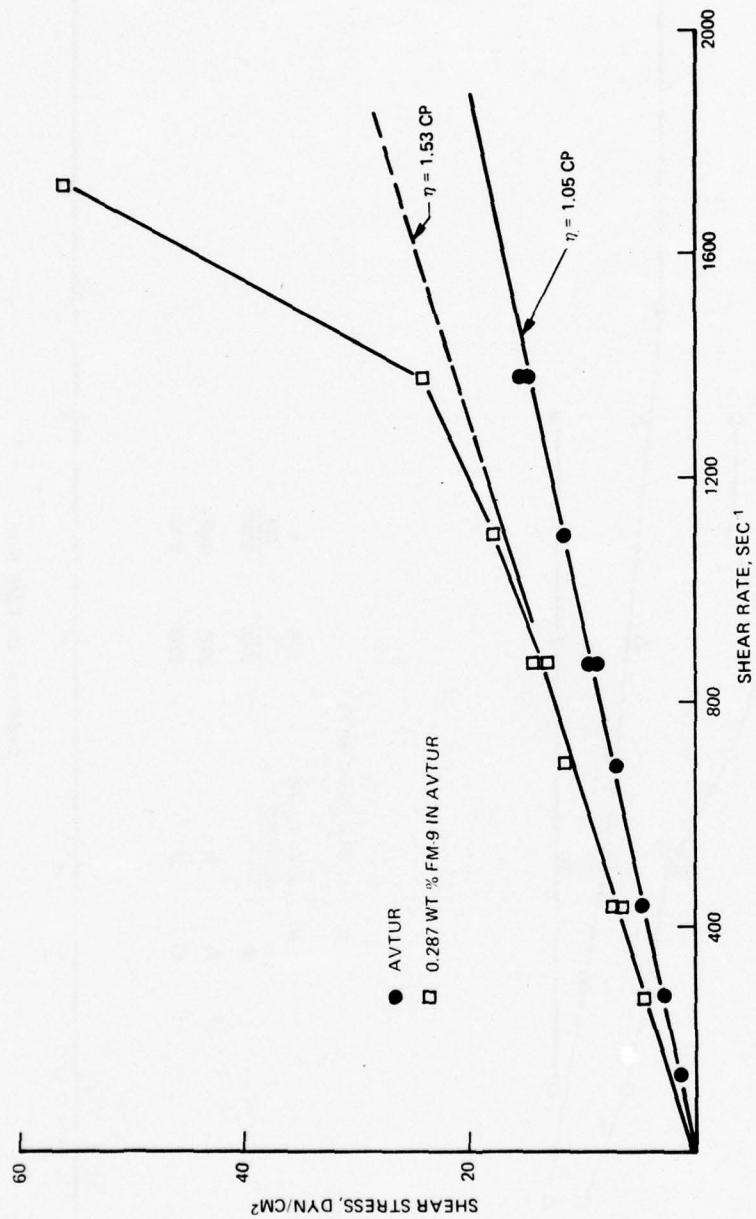


FIGURE 10. SHEAR THICKENING OF ANTIMIST FUEL (0.287 wt% FM-9 in Avtur) WITH A CONE (1°) AND PLATE VISCOMETER.

TABLE 2. CRITICAL SHEAR STRESS AT ONSET
OF SHEAR THICKENING (0.287wt% FM-9
in Avtur at 25-26°C)

<u>Critical Shear Stress</u> dyn/cm ²	<u>Viscosity Ratio</u> Dimensionless	<u>Apparatus</u>
44-59	1.4	Capillary Tube: R = 0.039 cm L/R = 2341
44-58	1.4	Capillary Tube: R = 0.031 cm L/R = 2026
26-34	1.6	Capillary Tube: R = 0.031 cm L/R = 2026
31-36	1.7	Capillary Tube: R = 0.031 cm L/R = 2026
26-37	1.6	Capillary Tube: R = 0.031 cm L/R = 1017
13-18	1.5	Rotational Viscometer: 1° cone
7-14	1.6	Rotational Viscometer: 1° cone

B. Intrinsic Viscosity

As was noted in the previous section, the shear viscosity of antimist fuels is generally a complex function of the shear rate (e.g., the shear viscosity decreased for AM-1 and first decreased and then increased for XD-8132.01 and FM-9). Even more important, the shear viscosity depends strongly on the polymer concentration; however, the intrinsic viscosity is a basic polymer property that is independent of concentration and is less sensitive to the shear rate and the temperature than the absolute viscosity. One does not measure the intrinsic viscosity directly. Instead two quantities defined as the reduced viscosity and inherent viscosity:

$$\eta_{\text{red}} \equiv (\eta_r - 1)/C \quad (3)$$

$$\eta_{\text{inh}} \equiv (\ln \eta_r)/C \quad (4)$$

are plotted as a function of the polymer concentration C . Under certain conditions these graphs will be essentially linear and extrapolate to a common intercept. The value of this intercept is taken as the intrinsic viscosity:

$$[\eta] \equiv \lim_{C \rightarrow 0} \eta_{\text{red}} \quad (5)$$

or

$$[\eta] \equiv \lim_{C \rightarrow 0} \eta_{\text{inh}} \quad (6)$$

Since the viscosity ratio is dimensionless, the intrinsic viscosity has the dimensions of reciprocal concentration and has traditionally been given in units of dl/gm. Ideally, these measurements should be made with extremely dilute solutions corresponding to $1.1 < \eta_r < 1.5$ and at very low shear rates.⁽¹⁾ However for AM-1 we have found less scatter in the data if concentrations were chosen so that $1.4 < \eta_r < 2.5$. Furthermore, because of the low viscosity of antimist fuels it is difficult to measure the shear viscosity at the very low shear rates that are required to accurately determine the zero shear rate viscosity of AM-1 solutions. While future work should consider the development of a low shear rate technique that is suitable to low viscosity liquids, for the present we have attempted to estimate the zero shear rate viscosity by extrapolating the shear viscosity measured with a four-bulb viscometer to zero shear rate. The reason for the choice of this instrument over the capillary viscometer described earlier is that it is much easier to provide for precise temperature control with the 4-bulb device. Intrinsic viscosities were also measured with a standard Cannon-Ubbelohde viscometer and a comparison of these two methods for AM-1 in JP-8 at $37.8^\circ\text{C} \pm 0.01^\circ\text{C}$ (100°F) is made in Figure 11. While it is evident that the intrinsic viscosities differ by about 40% (i.e., 14.0 and 10.0 dl/gm), because of the relative simplicity of the standard viscometer,

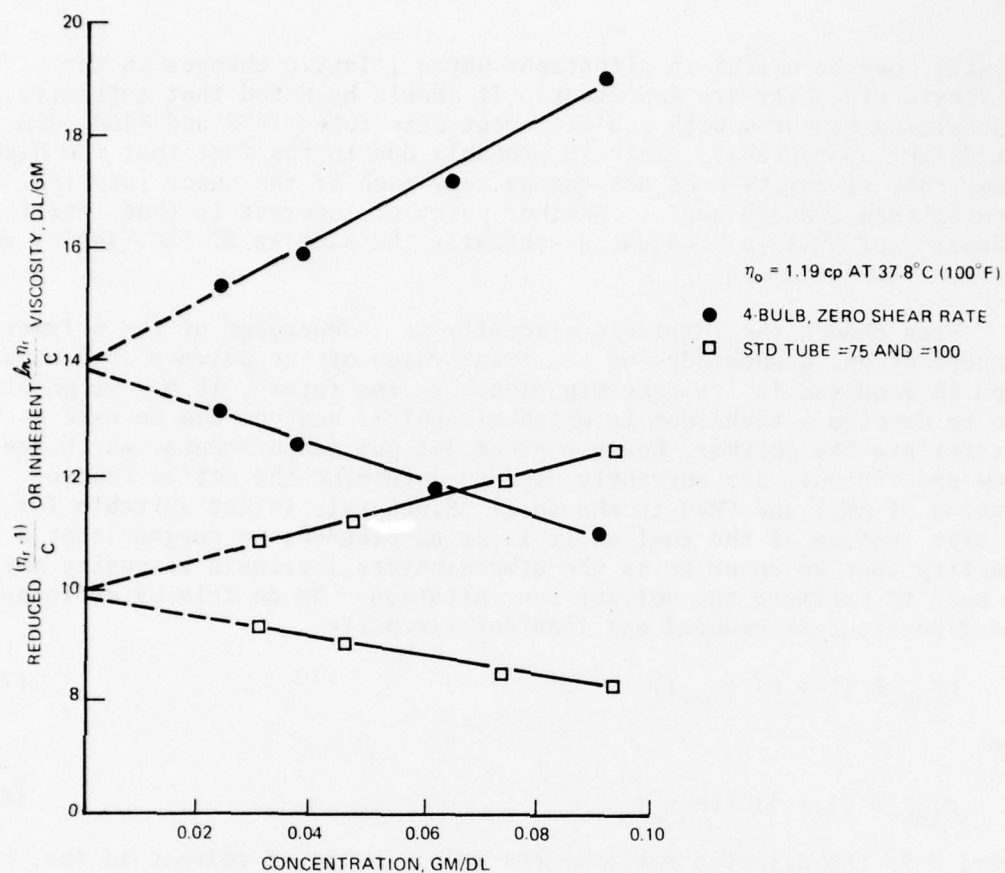


FIGURE 11. REDUCED OR INHERENT VISCOSITY OF AM-1 (AFLRL) IN JP-8 BY TWO DIFFERENT METHODS.

it still may be useful in situations where relative changes in the intrinsic viscosity are important. It should be noted that intrinsic viscosities measured with two different size tubes (#75 and #100) did not differ appreciably. This is probably due to the fact that the high shear rate viscosity does not change very much if the shear rate is greater than $200\text{-}300 \text{ sec}^{-1}$. Another point of interest is that intrinsic viscosity of AM-1 in JP-8 was essentially the same at 37.8°C (100°F) and at room temperature.

Even though the intrinsic viscosity is independent of the polymer concentration, a knowledge of the exact value of the polymer concentration is required in its determination. In the future, it may be possible to develop a technique in which alcohol or acetone can be used to precipitate the polymer, however steam jet gum measurements, which are slow and tedious, are currently used to determine the active concentration of AM-1 and FM-9 in the fuel. Since this is not suitable for on-site testing of the fuel as it is being blended, we suggest that a quantity that we refer to as the dimensionless intrinsic viscosity may be used to estimate the polymer concentration. We do this by defining the dimensionless reduced and inherent viscosity:

$$\eta_{\text{red}}^* \equiv (1 + \delta) (\eta_r - 1) \quad (7)$$

and

$$\eta_{\text{inh}}^* \equiv (1 + \delta) (\ln \eta_r) \quad (8)$$

where δ is the dilution ratio or the volume ratio of solvent to the volume of original solution at initial concentration C_0 . As with the previous definition, we take the dimensionless intrinsic viscosity to be the common intercept of:

$$[\eta^*] \equiv \lim_{\delta \rightarrow \infty} \eta_{\text{red}}^* \quad (9)$$

and

$$[\eta^*] \equiv \lim_{\delta \rightarrow \infty} \eta_{\text{inh}}^* \quad (10)$$

It should be noted that the dimensionless concentration ratio (C/C_0) is given by

$$C/C_0 = \frac{1}{(1 + \delta)} \quad (11)$$

The ratio between the dimensionless and conventional intrinsic viscosity is the polymer concentration in gm/dl:

$$C_0 = [\eta^*]/[\eta] \quad (12)$$

Thus, if we measure the dimensionless intrinsic viscosity and know the value of $[\eta]$, we can calculate the polymer concentration from equation 12. The data in Figure 12 were obtained with a standard viscometer over

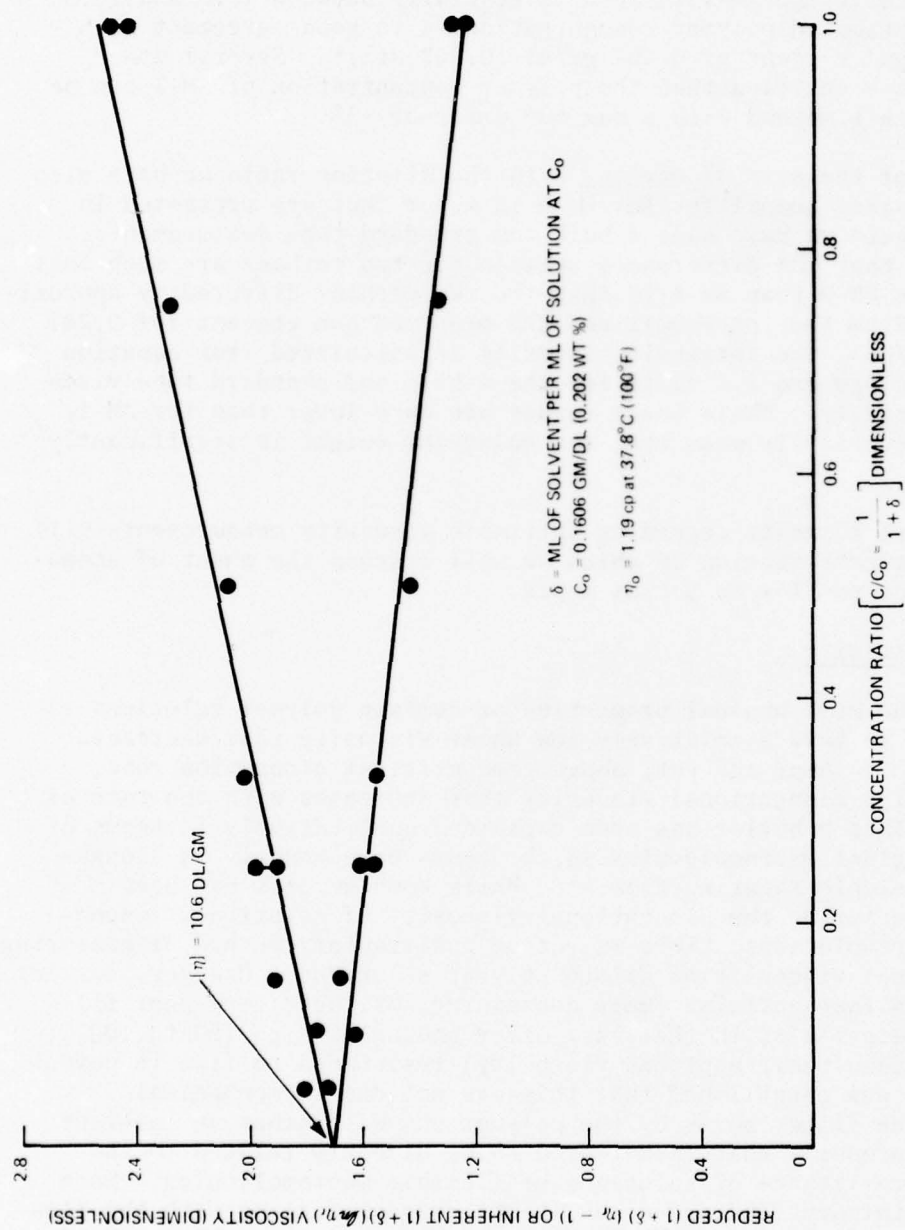


FIGURE 12. DIMENSIONLESS REDUCED OR INHERENT VISCOSITY OF AM-1 IN JP-8 (Std. Tube).

a very wide range of dilutions that corresponded to $1.09 < \eta_r < 2.5$. The common intercept of 1.7 is equivalent to a polymer concentration of $0.165 < C_0 < 0.170$ gm/dl which was calculated from the fact that the intrinsic viscosity of AM-1 in JP-8 is generally between 10.0 and 10.3 dl/gm. The estimated polymer concentration is in good agreement with the measured gum content of 0.161 gm/dl (0.202 wt%)*. Several other experiments have verified that the polymer concentration of AM-1 can be estimated by this method with a maximum error of +3%.

Because of the ease of working with the dilution ratio we have also used dimensionless quantities for FM-9 in Avtur that are presented in Figure 13. Again we have made 4-bulb and standard tube measurements. It is evident that the differences between the two methods are much less important with FM-9 than AM-1 in that the two methods differed by approximately 10%. From the intercepts and the measured gum content (of 0.287 wt% (0.221 gm/dl), the intrinsic viscosity is calculated from equation 12 to be 2.2 dl/gm and 2.0 dl/gm for the 4-bulb and standard tube viscometers respectively. While these values are much lower than for AM-1, they do not necessarily mean that the molecular weight is significantly lower.

Additional comments regarding intrinsic viscosity measurements will be made in the next section in which we will discuss the onset of anomalous resistance to flow in porous media.

C. Viscoelasticity

One of the most unusual properties of certain polymer solutions is their ability to have a relatively low shear viscosity that decreases with the rate of shear and yet, above some critical elongation rate, have a very high elongational viscosity that increases with the rate of elongation. This behavior has been explained qualitatively in terms of uncoiling of giant macromolecules which occurs more readily in elongation than in simple shearing flow.⁽²⁾ While some success has been achieved in measuring the elongational viscosity of relatively concentrated polymer solutions, there is yet no satisfactory method of measuring the elongational viscosity of dilute polymer solutions. However, earlier work has shown that antimist fuels containing AM-1 have very poor filtration characteristics in that they offer unusually high (50 to 100 times higher than their apparent viscosity) resistance to flow in porous media.⁽³⁾ It was established that this was not due to mechanical blockage of the filter pores by the polymer but was rather an inherent viscoelastic property that is believed to be directly related to the elongational resistance of solutions of flexible macromolecules. More recently preliminary findings of an ILIR** program dealing with the flow of dilute polymer solutions in porous media indicate that the onset of this anomalous resistance is in fact a viscoelastic phenomenon in that

* C_0 (gm/dl) = ρ (gm/dl) · wt%, ρ_{JP-8} = 0.795 gm/ml at 37.8°C, ρ_{AVTUR} = 0.771 gm/ml at 37.8°C.

**An In-House Laboratory Independent Research program, sponsored by U.S. Army Mobility Equipment Research and Development Command, April 24, 1976.

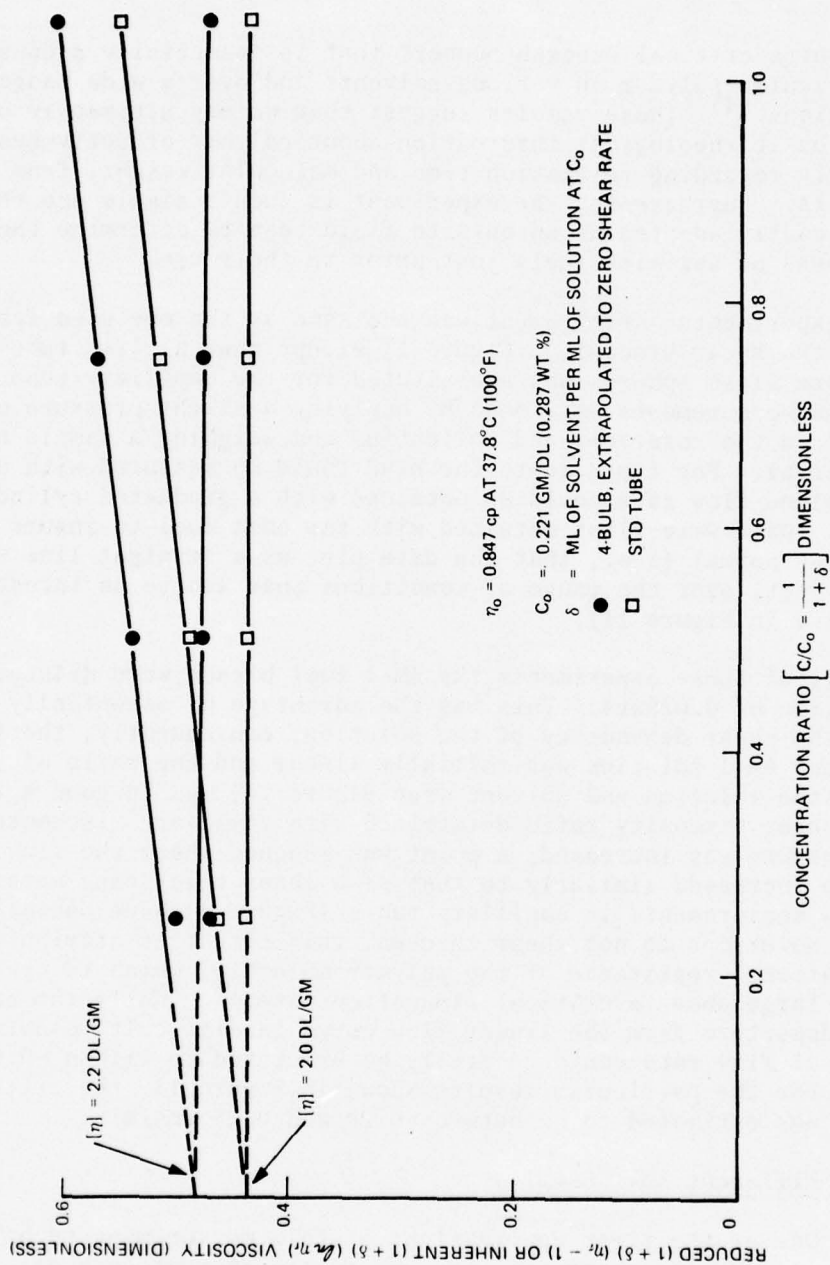


FIGURE 13. DIMENSIONLESS REDUCED OR INHERENT VISCOSITY OF FM-9 IN AVTUR BY TWO DIFFERENT METHODS.

it occurs at a critical Deborah number* that is essentially a constant for a particular polymer in various solvents and over a wide range of concentrations.⁽⁴⁾ These results suggest that we may ultimately be able to obtain basic rheological information about polymer effectiveness, particularly regarding relaxation time and molecular weight, from these measurements. Furthermore, the experiment is such a simple one that it could be readily adopted as an on-site field test to determine the effectiveness of antimist fuels just prior to their use.

The experimental arrangement was the same as the one used for measuring the shear viscosity (Figure 1) except that a glass tube filled with uniform glass spheres was substituted for the capillary tube. Again, flow measurements were made by applying a slight pressure or fluid head to the reservoir and collecting and weighing a sample over a timed interval. For field tests the head could be measured with a ruler and the volume flow rate could be obtained with a graduated cylinder and stopwatch. Data were first obtained with the base fuel to insure that the flow was normal (i.e., that the data plot as a straight line with zero intercept) over the range of conditions that are to be investigated (lower curve in Figure 11).

In all of these experiments the AM-1 fuel blends were diluted to a concentration of 0.025wt%. This has the advantage of essentially eliminating the shear dependency of the solution; consequently, the flow curve of the AM-1 solution was initially linear and the ratio of the slopes of the solution and solvent (see Figure 14) was in good agreement with the shear viscosity ratio determined with capillary viscometers. As the pressure was increased, a point was reached where the flow resistance increased similarly to that of a shear thickening material. Since flow measurements in capillary tubes (Figure 4) have established that AM-1 solutions do not shear thicken, this effect is attributed to the elongational resistance of the polymer molecule, which is predicted to become large above a critical elongation rate.⁽⁵⁾ While the exact point of departure from the linear flow curve is difficult to determine, the critical flow rate could generally be bracketed to within ± 0.05 gms/min. For the particular results shown in Figure 14, the critical flow rate was estimated to be between 0.20 and 0.25 gms/min.

1. Different AM-1 Samples

One of the first applications of this measurement technique was comparing AM-1 concentrates obtained from different sources: Dynamic Sciences, National Aviation Facilities Experimental Center (NAFEC), U.S. Army Fuels and Lubricants Research Laboratory (AFLRL), Naval Air Propulsion Test Center (NAPTC), and Jet Propulsion Laboratory (JPL). The gum content of each solution was measured to insure that it contained the same amount of AM-1. The results presented in Figure 15 show that there are major differences in solutions made from these samples as reflected

*The Deborah number is a dimensionless parameter that indicates the relative importance of elastic to purely viscous forces.

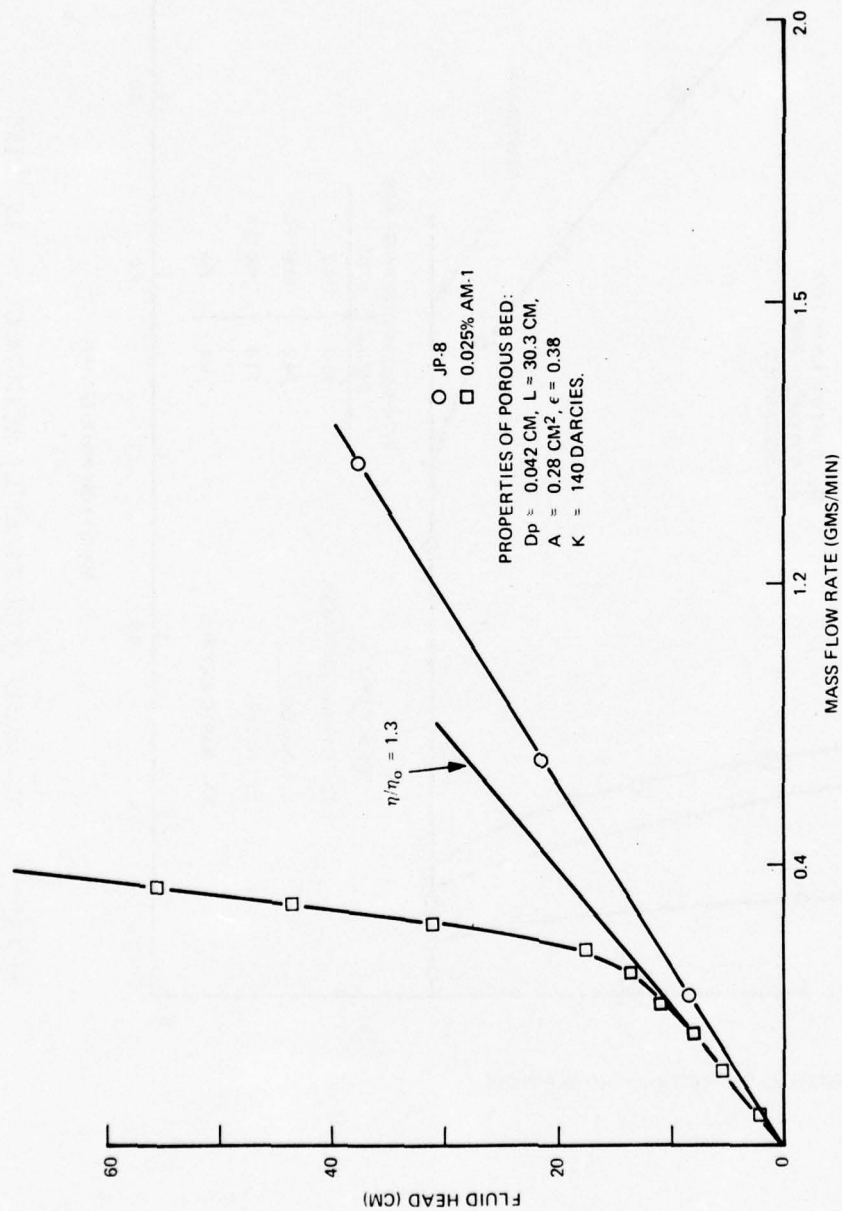


FIGURE 14. DETERMINATION OF ONSET OF ANOMALOUS (VISCOELASTIC) RESISTANCE OF DILUTE AM-1 SOLUTION TO FLOW IN POROUS MEDIA.

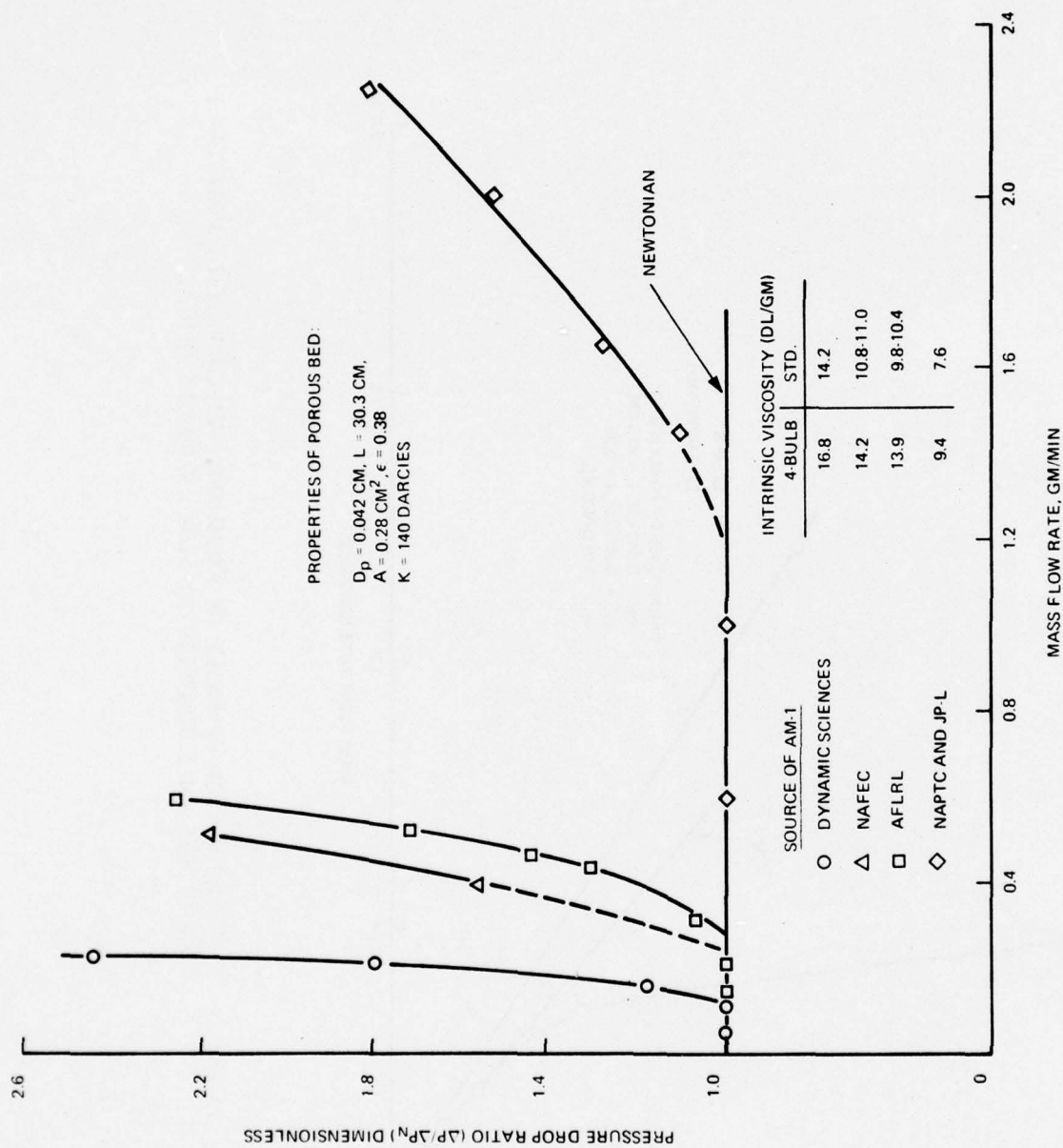


FIGURE 15. ANOMALOUS (VISCOELASTIC) RESISTANCE OF ANTIMIST FUELS MADE WITH AM-1 FROM DIFFERENT SOURCES.

by the different flow rates at the onset of anomalous resistance in porous media. These data were obtained from flow curves similar to Figure 14; however, the results are expressed in terms of a dimensionless pressure ratio ($\Delta P/\Delta P_N$) that is unity for all flow rates below critical. The intrinsic viscosities of these samples also varied significantly, however these differences were not nearly as large as the differences in the critical flow rate, i.e.,

$$\frac{[\eta]_{\max}}{[\eta]_{\min}} = \frac{14.2}{7.6} \approx 2, \quad \frac{(W_c)_{\max}}{(W_c)_{\min}} \approx \frac{1.0}{0.1} = 10$$

Thus the critical flow rate appears to be much more sensitive to differences in viscoelasticity and is actually easier to measure than intrinsic viscosity. Later we will show the theoretical basis for the apparent correlation between the intrinsic viscosity and the critical flow rate and why the former should generally be expected to be less sensitive than the latter. It is presently felt that these observed differences can be attributed to the AM-1 samples being from different batches. While it is not known how important these differences are to mist flammability, recent fuel spillage/air shear tests conducted at the NWC indicate that the AM-1 from AFLRL, which had a higher intrinsic viscosity and a lower critical flow rate, also appears to be safer than the newer AM-1 from NAPTC.

2. Effect of Blending

The second application of determining the onset of anomalous resistance to flow in porous media was in showing the importance of using a proper blending technique in order to prevent mechanical degradation of the AM-1 additive. The results shown in Figure 16 are for AM-1 (NAFEC) blended in Jet-A with a lab stirrer (magnetic) for approximately 30 minutes at room temperature and a sample that was blended at Naval Weapons Center (NWC) by recirculating through a pump (centrifugal pump, 1 hp, 3450 RPM, 10 gal/min) for 14 to 16 hours at a temperature of approximately 100°F. Intrinsic viscosity measurements indicated that the polymer had been partially degraded; however, much larger differences were evident in the porous media experiment:

$$\frac{[\eta]_{\text{stirred}}}{[\eta]_{\text{pumped}}} = \frac{11.0}{7.6} \approx 1.4 \quad \text{whereas} \quad \frac{(W_c)_{\text{pumped}}}{(W_c)_{\text{stirred}}} = \frac{4}{0.2} = 20$$

Attempts to characterize the molecular weight distribution of these two samples produced rather unusual results in that the high molecular weight fractions of the pumped sample were larger than the stirred sample:

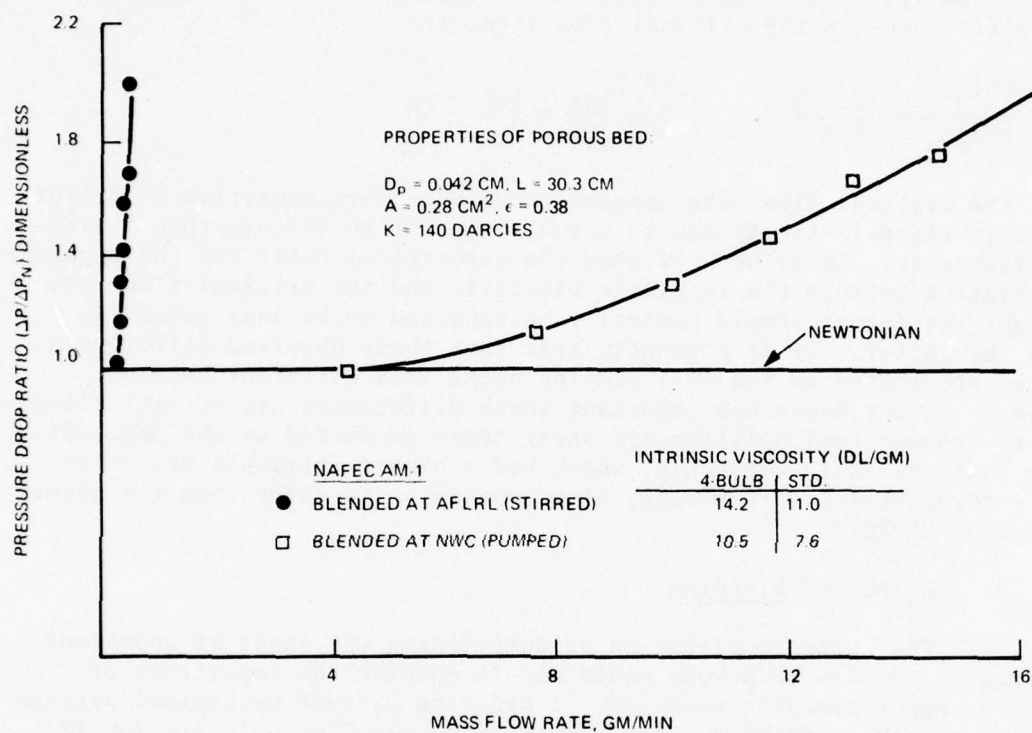


FIGURE 16. EFFECT OF BLENDING TECHNIQUE ON ANOMALOUS (VISCOELASTIC) RESISTANCE OF ANTIMIST FUELS.

	GPC Molecular Weight Distribution*						
	>5m	5m to 2m	2m to 1m	1m to 500K	500K to 200K	200K to 100K	
NAFEC (AM-1)							
stirred	7	24	24	18	16	7	4
pumped	22	34	17	11	11	3	-
pumped	24	40	19	10	7	-	-

Although mechanical degradation normally results in a lower molecular weight, particularly in the high molecular weight fractions, it is possible that chain-branching or a slight degree of cross-linking may have followed chain-breaking. This is more likely to occur at elevated temperatures (the pumped samples were heated to 100°F and may have risen above this value) and could account for the increased molecular weight. Furthermore, since branched or slightly crosslinked polymers generally result in a much lower intrinsic viscosity and reduced flexibility, this could readily explain the apparent anomaly of increased molecular weight but reduced intrinsic viscosity and viscoelasticity.

Mist flash-back⁽⁶⁾ measurements of the pumped and stirred antimist fuels showed no measurable differences, except that burning downstream of the pilot flame was observed only for the pumped sample. While this is not a part of the current test procedure, it is felt that it is indicative of poorer antimist protection. Furthermore, since the mist flash-back test was also unable to discriminate between antimist fuels made with AM-1 from AFLRL and NAPTC, it appears that the test in its current configuration is not severe enough to simulate the mist forming conditions in a fixed-wing aircraft crash. Because of flame blow-off, it does not appear possible to increase the intensity of the air-shear in the mist flash-back test, however it was suspected that flash-back differences would be observed if measurements were made at series of dilutions. Unfortunately there wasn't enough of the pumped antimist fuel left for these experiments. However, significant differences had been observed for the intrinsic viscosities and critical flow rates of solutions made with samples of AM-1 from AFLRL and NAPTC; consequently, these solutions were used.

The results in Figure 17 show that at the higher concentration of 0.20 and 0.10 wt% AM-1, the flash-back was identical for both samples; however at intermediate concentrations of 0.05 and 0.025 wt% the flash-back for the NAPTC AM-1 was higher. The fact that a maximum difference was noted at the intermediate concentration of 0.05 wt% is reasonable in light of the fact that the two solutions must also have the same flash-back at zero concentration. The higher flash-back for the dilute NAPTC solution is in agreement with the intrinsic viscosity and critical flow rate measurements and indicates that the antimist fuel made with the AFLRL AM-1 should offer better fire protection. Furthermore, these

*Gel Permeation Chromatography data was obtained with a Waters -100 (ALC) High Performance Liquid Chromatograph, using polystyrene (Max MW = 3.5×10^6) as the standard and THF as the solvent.

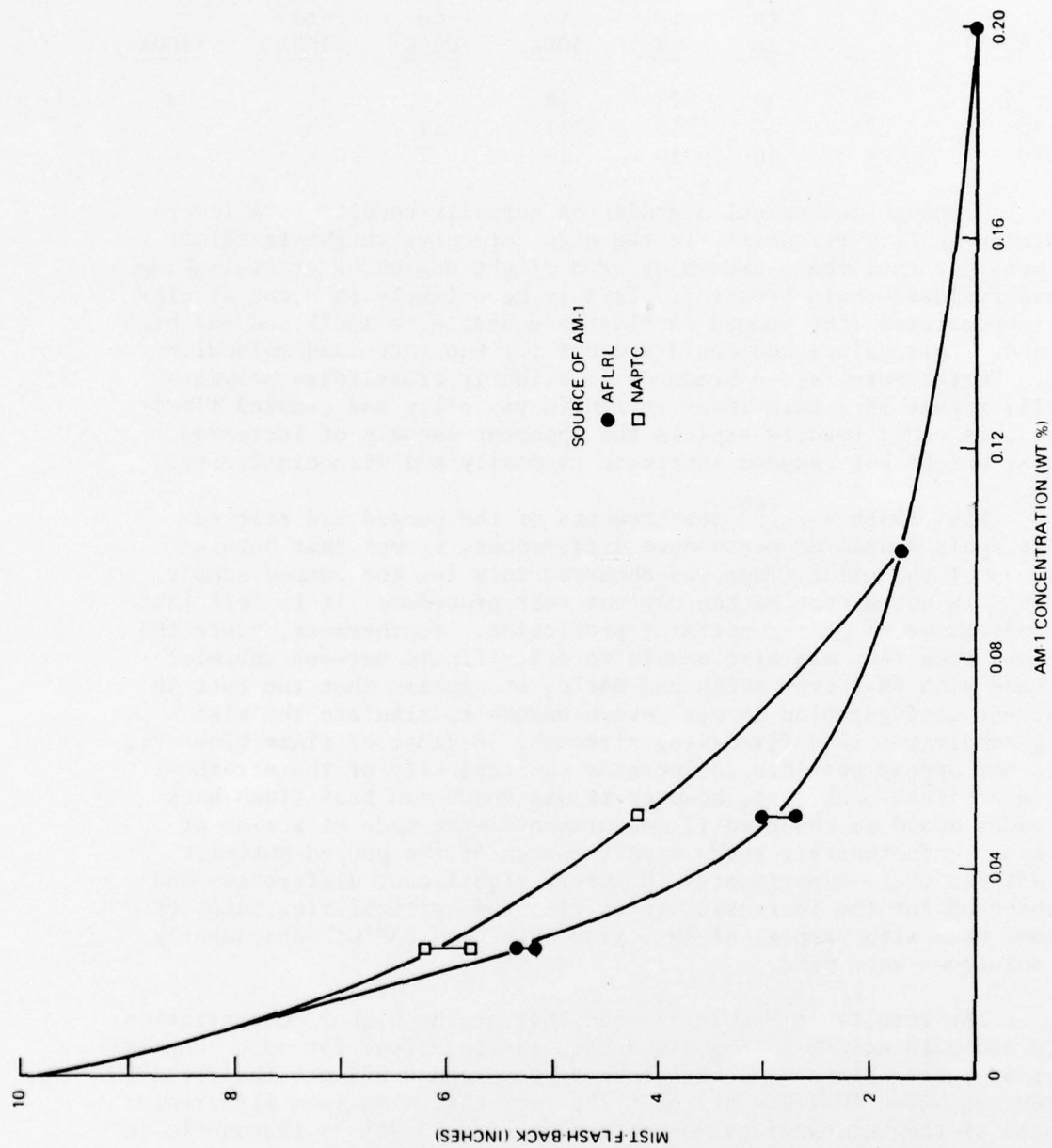


FIGURE 17. EFFECT OF CONCENTRATION ON MIST-FLASH-BACK OF ANTIMIST FUELS (AM-1 in JP-8) FROM AFLRL AND NAPTC.

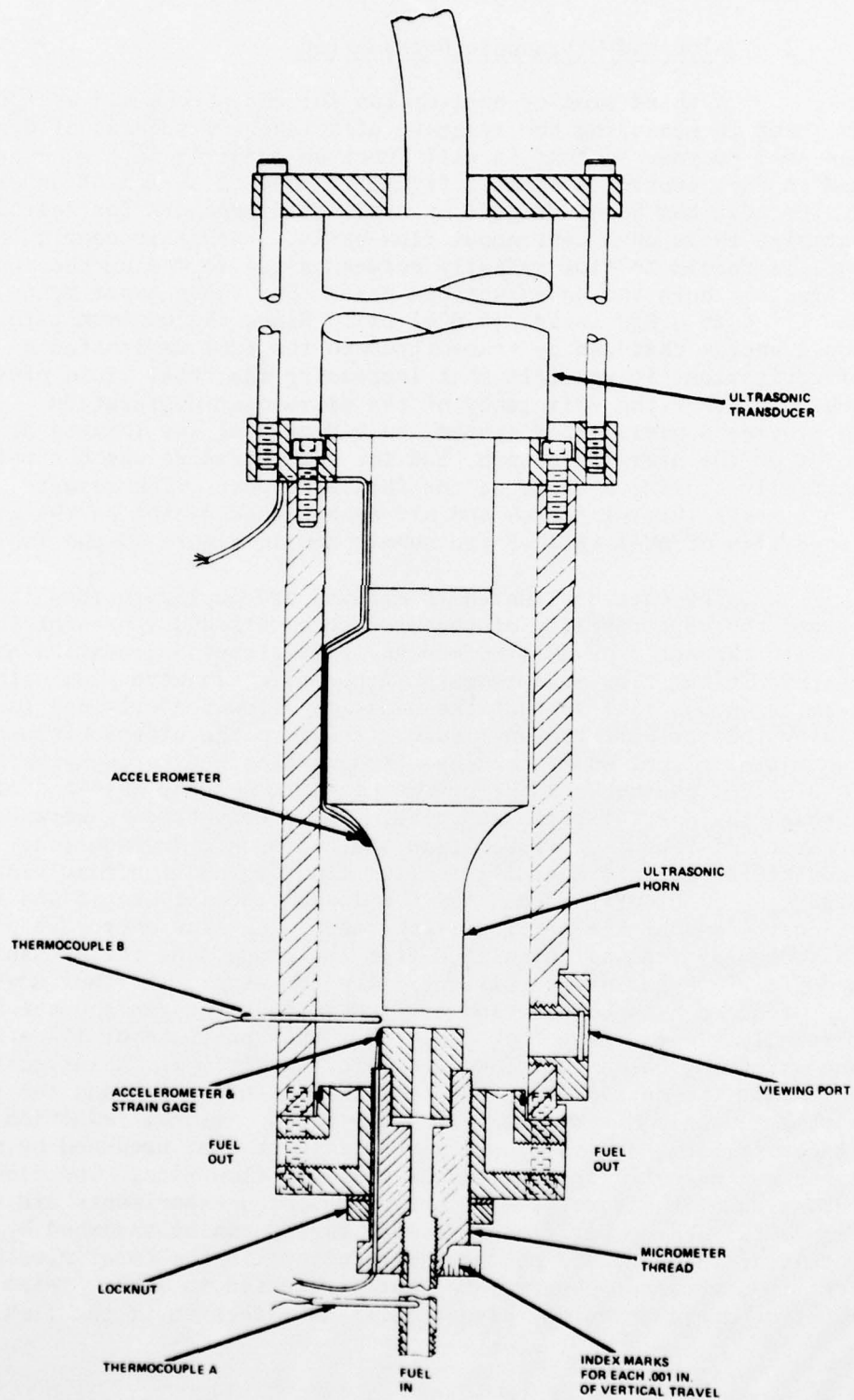
results suggest that the flash-back of the pumped fuel would have been greater than the one made with the NAPTC AM-1 if measurements would have been made at several concentrations lower than 0.20 wt%.

3. Flow and Ultrasonic Degradation

A third area of application for the porous media experiments has been in measuring the relative efficiency of methods of degrading the AM-1 polymer so that it will function properly in engine starting and in fuel control systems. Figure 18 shows a sketch of an ultrasonics device that has been designed by AFLRL staff members for degrading antimist fuels on a continuous flow basis. With this configuration, the fuel is forced to flow radially between a gap formed by the top of the ultrasonic horn and an adjustable base. For these experiments the gap was fixed at 0.030 inches (0.0762 cm). Since the maximum rate of ultrasonic energy that can be transmitted to the fuel is limited by the onset of cavitation, it was felt that increasing the total fluid pressure would increase the efficiency of the ultrasonic degradation. In order to provide a pressurized system, an O-ring seal was located at the null-point of the ultrasonic horn, and the back pressure was controlled by partially closing a valve at the fuel exit port. The results of the experiments involving flow and ultrasonic degradation on the rheological properties of AM-1 in JP-8 are summarized in Figure 19 and Table 3.

The data designated (0 ml/min) are duplicate runs that demonstrate the repeatability of these measurements and represent the viscoelastic character of AM-1 before any significant degradation has occurred. Again critical flow measurements in porous media were made with diluted samples (0.025 wt%) so that the behavior below the critical was essentially that of a Newtonian liquid. Prior to the ultrasonic experiments, the antimist fuel was forced by nitrogen pressure through the 0.03" (0.0762 cm) gap between the ultrasonic horn and the base and also through the partially closed valve. These measurements were made in order to distinguish between flow and ultrasonic degradation. The sensitivity of this antimist fuel to flow degradation resulting from the 0.03" gap is clearly evident by the lower viscosity ratio and intrinsic viscosity and higher critical flow rate. The flow energy to produce this degradation was calculated from the product of the pressure drop and flow rate and was surprisingly low (5 watts). Further degradation was produced by a combination of flow through the gap and through a partially closed valve that produced a back pressure of 1.4 atm (20 psi) and which increased the flow energy to 8 watts. It is interesting to note that the degradation resulting from both the gap and the valve (8 watts) had only a very small (roughly 2%) additional reduction on the viscosity ratio and intrinsic viscosity over that produced by the gap alone but essentially doubled the critical flow rate. The flow characteristics of the samples from the ultrasonics experiments are also in Figure 19. These verified that more energy can be absorbed by the fuel, resulting in increased polymer degradation, if the total pressure of the fuel is increased; however, the data presented in Table 3 also suggest the flow degradation may also be just as effective if the flow energy is

FIGURE 18. ULTRASONIC DEVICE FOR
DEGRADING ANTIMIST FUELS.



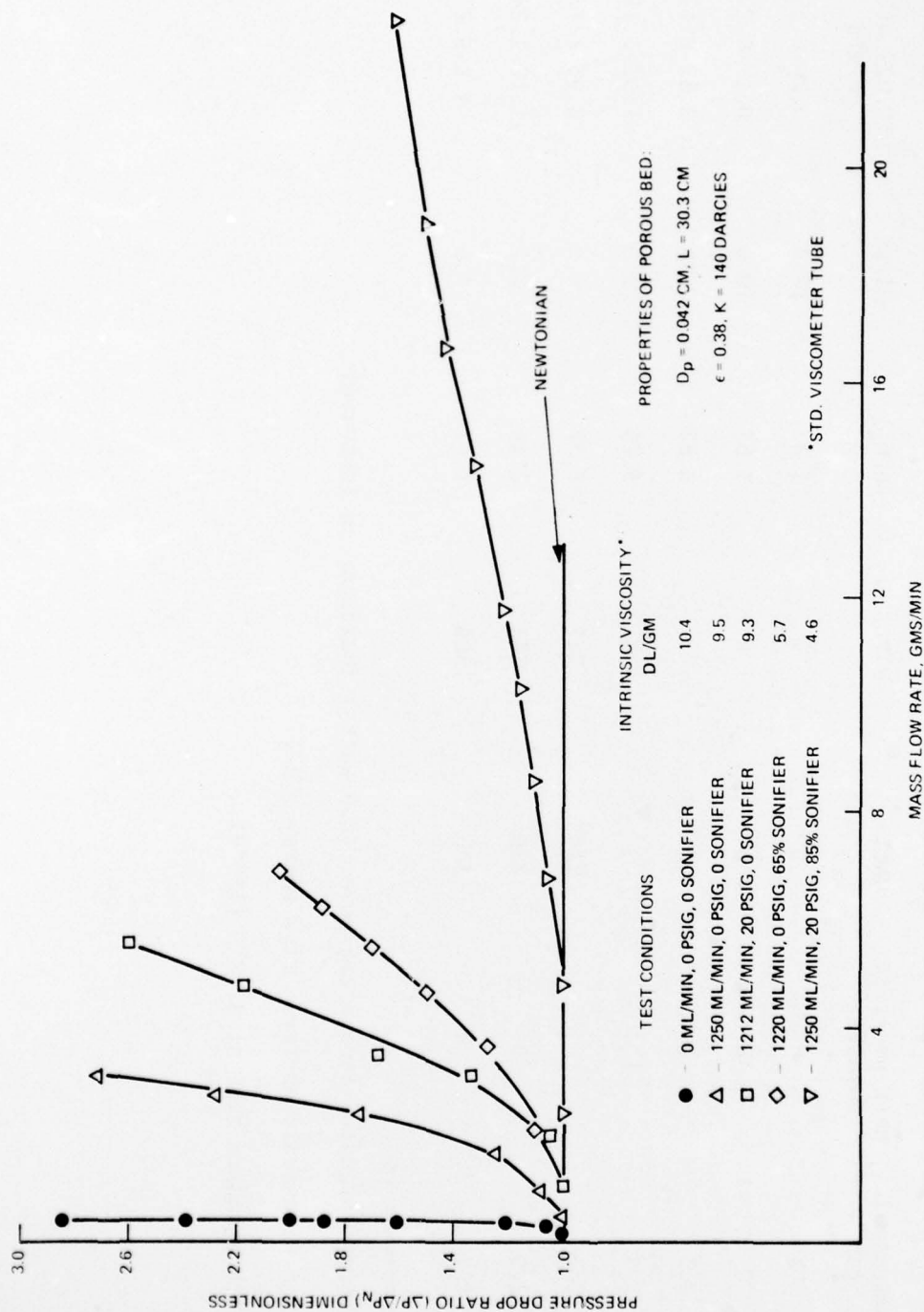


FIGURE 19. EFFECT OF FLOW AND ULTRASONIC DEGRADATION ON THE ANOMALOUS (VISCOELASTIC) RESISTANCE OF ANTIMIST FUELS (0.025 wt% AM-1 in JP-8) TO FLOW IN POROUS MEDIA.

TABLE 3. EFFECT OF FLOW AND ULTRASONIC DEGRADATION ON RHEOLOGICAL PROPERTIES
OF ANTIMIST FUEL (0.20 wt% in JP-8) AM-1

Flow Rate	Pressure Drop (atm)		Total Energy		Viscosity Ratio***	Intrinsic Viscosity***	Critical Flow Rate
	ultrasonic gap	back pressure valve	Ultrasonic Energy*	Dissipation**			
ml/min			watts	watts	(η/η_0)	dl/gm	(0.025 wt%) gm/min
0	0	0	0	0	3.47	10.3	0.20-0.25
0	0	0	0	0	3.53	10.6	0.17-0.27
1250	2.3	0	0	5	3.32	9.5	0.52-0.67
1212	2.3	1.4	0	8	3.25	9.3	1.05-1.15
1220	2.3	0	210	215	2.37	6.2	0.93-1.13
1220	2.3	0	230	235	2.24	5.7	1.12-1.24
1250	2.3	1.4	300	308	1.97	4.6	4.8-5.2

*Ultrasonic energy estimated from % max power (350 watts) indicator on instrument.

**Total energy = ultrasonic energy + flow energy (VAP).

***Measured with standard tube at 37.8°C (100°F).

increased to the same level as the ultrasonic energy. These conclusions are only tentative in that other factors such as flow rate, gap size and back pressure need to be studied in more depth. Furthermore, a more precise measurement is needed for the actual power consumption of the ultrasonic device than is provided by the system in its present form.

4. Theoretical Significance of the Critical Flow Rate

Up to this point we have said very little concerning the theoretical significance of the critical flow rate; however, as was mentioned earlier, the results of an ongoing ILIR program indicate that the onset of anomalous resistance in porous media occurs at a critical Deborah number

$$N_{Deb}^* = \Theta \dot{\gamma}_e \quad (13)$$

where N_{Deb}^* is the value of the Deborah number at onset,
 Θ is the relaxation time of the polymer solution, and
 $\dot{\gamma}_e$ is the elongation rate.

Although polymer solutions exhibit a distribution of relaxation times, the maximum Rouse⁽⁷⁾ relaxation time, which is a measure of the time for a polymer molecule to return to an unstressed configuration after it has been deformed, can be calculated from:

$$\Theta = \frac{6 (\eta_r - 1) \eta_o M}{\pi^2 C R T} \quad (14)$$

where η_r is the relative viscosity or viscosity ratio of solution to solvent,

η_o is the viscosity of the solvent,

M is the molecular weight of the polymer,

C is the concentration of the polymer,

R is the gas constant, and

T is the absolute temperature.

Also, while the elongation rate in a porous bed cannot be measured directly, for a bed consisting of uniform spheres, it can be estimated from the flow rate by⁽⁸⁾:

$$\dot{\gamma}_e \approx \frac{150W}{AD_p \rho} \quad (15)$$

where W is the average mass flow rate,

A is the cross-sectional area,

D_p is the diameter of the sphere, and

ρ is the density of the solution.

For dilute solutions of polyisobutylene (Vistanex L-200) in several pure solvents and over a wide range of concentrations, it was found that the critical Deborah number was approximately a constant,

i.e., $1.0 < N_{Deb}^* < 2.0$. Similar measurements for AM-1 in JP-8 and diesel fuel indicate that the critical Deborah number is also a constant at onset or equivalently, at a fixed concentration, that the product of the viscosity ratio, the solvent viscosity and the critical flow rate is a constant:

$$[(\eta_r - 1)\eta_o W_c]_{JP-8} \approx [(\eta_r - 1)\eta_o W_c]_{DF-2} \quad (16)$$

However the exact value of the critical Deborah number is not known due to the lack of information concerning the molecular weight of AM-1. Future plans of the basic research program are aimed at determining if $1.0 < N_{Deb}^* < 2.0$ for a relatively large class of structurally similar polymers, which would allow us to calculate the effective relaxation time and molecular weight from a measurement of the critical flow rate. For example, if the critical Deborah number is approximately 1.0 for dilute AM-1 solutions, then, from equations 13, 14 and 15, the relaxation times and molecular weights for the samples of AM-1 from different sources are:

Source of AM-1	Largest Relaxation Time* (sec)	Average Molecular Weight**
Dynamic Sciences	0.029	43×10^6
NAFEC	0.019	33×10^6
AFLRL	0.015	28×10^6
NAPTC	0.0034	9×10^6

While these values of the molecular weights seem to be higher than we might have expected, it must be remembered that the relaxation time, from which the molecular weight was calculated, is very strongly influenced by the high molecular fraction of AM-1. These estimates must be considered highly tentative until further research has established the general applicability of this approach; however it is hoped that this may be accomplished in the near future.

Finally, we wish to show the theoretical basis for the general observation that if the critical flow rate of a solution containing AM-1 increases there will be a much smaller but measurable decrease in the intrinsic viscosity. In order to establish this relation, it should be recalled that the term $(\eta_r - 1)/C$ in equation 14 is the reduced viscosity and that at very low concentrations this quantity has approximately the same value as the intrinsic viscosity; consequently, equation 14 can be written as

$$\Theta \approx \frac{6 [\eta] \eta_o M}{\pi^2 R T}, \quad C \approx 0 \quad (17)$$

Calculated from equations 13 and 15, assuming $N_{Deb}^ = 1.0$.

**Calculated from equation 14.

For linear polymers the intrinsic viscosity is related to the molecular weight by the following semi-empirical equation:

$$[\eta] = K M^a \quad (18)$$

where K and a are constants for a particular polymer that must be determined experimentally for each solvent. Furthermore, if it is assumed that at the onset of anomalous resistance the critical Deborah number is a constant, which we denote as N_{Deb}^* , then from equations 13, 15, 17 and 18, we have:

$$\frac{6 \eta_o [\eta]^{1+1/a}}{\pi^2 R T K^{1/a}} \cdot \frac{150 W_c}{A \rho D_p} = N_{Deb}^* \quad (19)$$

For a fixed bed geometry, polymer species and solvent, most of these terms are constants that can be collected together so that equation 19 can be written simply as

$$[\eta]^{1+1/a} = \alpha (1/W_c) \quad (20)$$

where α contains all of the constant terms. This can be solved for the intrinsic viscosity to yield

$$[\eta] = [\alpha(1/W_c)]^{a/1+a} \quad (21)$$

Equation 21 predicts that intrinsic viscosities and critical flow rate data should plot as a straight line with slope equal to $a/1+a$ if we plot $\log [\eta]$ Vs $\log [1/W_c]$. Figure 20 includes data that we have obtained on AM-1 samples from different sources and on samples of AM-1 that have been partially degraded with flow and/or ultrasonic energy. The best straight line through all the data has a slope of $1/3$ which is equivalent to $a = 1/2$. It should be noted that for the majority of linear polymers $0.5 \leq a < 0.8$. Since the lower number is the theoretical theta value, these results indicate that JP-8 is a relatively poor solvent for AM-1. Furthermore, the exponent of the critical flow rate ($a/1+a = 1/3$) explains why the intrinsic viscosity will generally be a less sensitive measure of degradation than the critical flow rate.

D. Physical Properties of Antimist Fuels (0.30% AM-1 in Jet-A) Used in Fuel Spillage/Air Shear Tests*

1. Comparison of AFLRL and NAPTC AM-1 Samples Blended at NWC

Antimist fuels containing AM-1 were blended at the test site in a 55 gallon drum by stirring for a period of one to two hours at a speed of 100 RPM with the fuel temperature at approximately 22 to 25°C. The design and size of the stirring blades were essentially the same as

*These tests were conducted at NWC, China Lake, California on October 13-20, 1976.

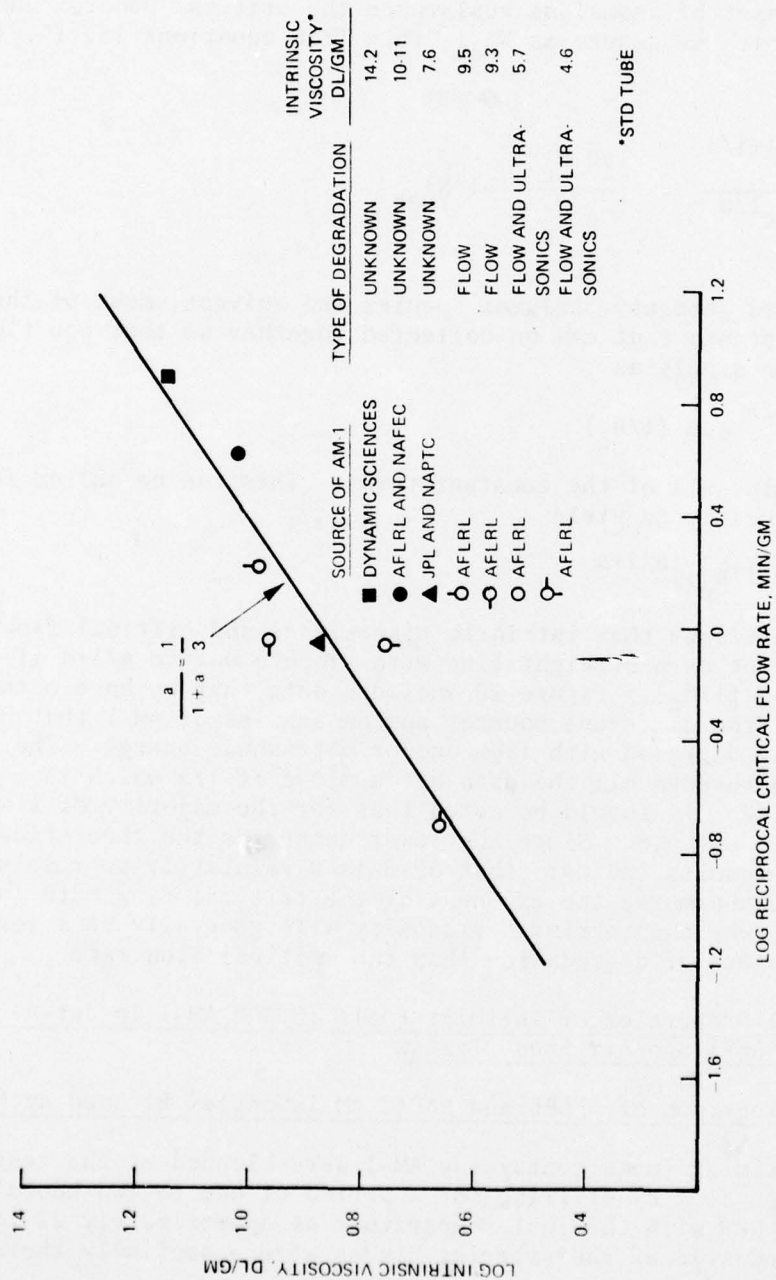


FIGURE 20. CORRELATION OF CRITICAL FLOW RATE IN POROUS MEDIA AND INTRINSIC VISCOSITY* FOR PARTIALLY DEGRADED ANTIMIST FUELS (0.025 wt% AM-1 in JP-8).

previously used by NAFEC and AFLRL in blending large volumes of antimist fuel. Intrinsic viscosity and critical flow rate measurements were determined for two antimist fuels made with the AFLRL AM-1 and one that was made with the NAPTC AM-1. All three fuels were blended to a concentration of 0.30 wt% AM-1 which was later verified by gum content. All of the viscosity data was obtained with a standard Cannon-Ubbelohde viscometer. The fuel temperature for the viscosity measurements was normal 37.8°C (100°F); however, some data were obtained at NWC by measuring the viscosity of the solution and the solvent simultaneously without any specific control over the temperature. Critical flow rates were made at room temperature with samples diluted to 0.025 wt%. The results of the experiments presented in Figures 21 and 22 show that the intrinsic viscosities and critical flow rates of the antimist fuels blended at NWC with AFLRL AM-1 and NAPTC AM-1 are in good agreement with values reported earlier (Figure 15) for samples blended at AFLRL with a small laboratory (magnetic) stirrer. These results also show that the intrinsic viscosity of AM-1 is essentially independent of the temperature for these conditions and that it can be measured without precise temperature control. Furthermore, it is evident that the intrinsic viscosity of the AFLRL AM-1 is higher than the NAPTC AM-1 and conversely, the critical flow rate of the former is lower than the latter. In light of this fact, it is important to again comment that fuel-spillage/air-shear tests results with these antimist fuels indicate that the AFLRL AM-1 provides significantly better fire protection; however it must be remembered that these conclusions are based on the results of only one test.

Conclusions and Recommendations

1. Below a critical shear stress, the viscosity of antimist fuels containing either XD-8132.01 or FM-9 was almost Newtonian, however above a critical shear stress these same fuels exhibited large magnitude shear thickening effects. Unfortunately, the flow rate of FM-9 was also time dependent. While it is not practical to obtain the value of the shear viscosity with capillary viscometers in this antithixotropic regime, it is felt that this simple procedure may be able to estimate the critical stress required to initiate the shear thickening phenomenon. This in itself may prove to be an important rheological parameter that can be used to determine the relative effectiveness of this additive, however additional work will be required for its development before it could be used as part of an antimisting fuel specification.
2. The shear viscosity of antimist fuels made with AM-1 decreases with the shear rate and does not appear to be directly responsible for the antimisting action; however these fuels do exhibit a very high resistance to flow in porous media. This phenomenon is not due to physical blockage of the pores but is a characteristic behavior of viscoelastic liquids. By working with very dilute solutions, it has been shown that the high resistance to flow in porous media occurs at a critical flow rate that appears to be related to the relaxation time of the solution.

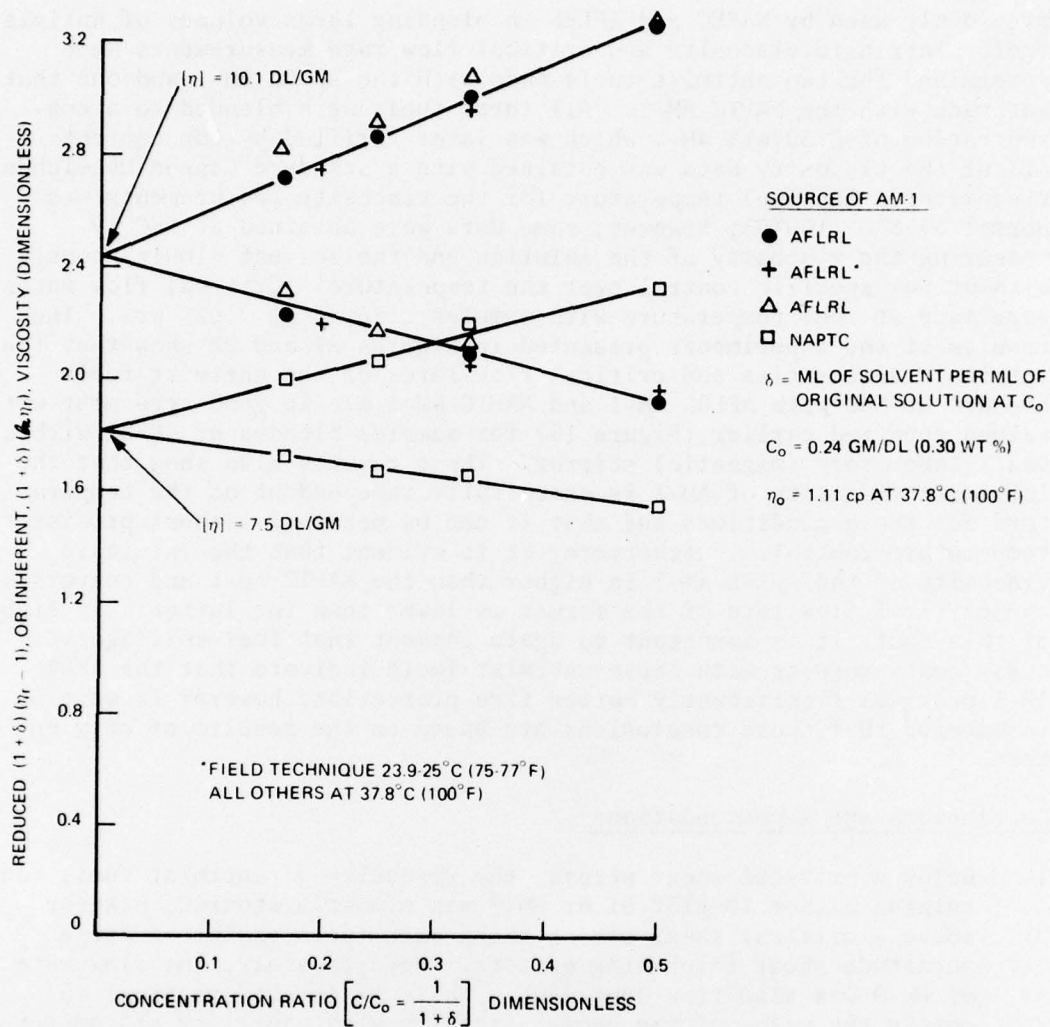


FIGURE 21. INTRINSIC VISCOSITIES OF ANTIMIST FUELS USED IN FUEL SPILLAGE/AIR SHEAR TESTS AT NWC.

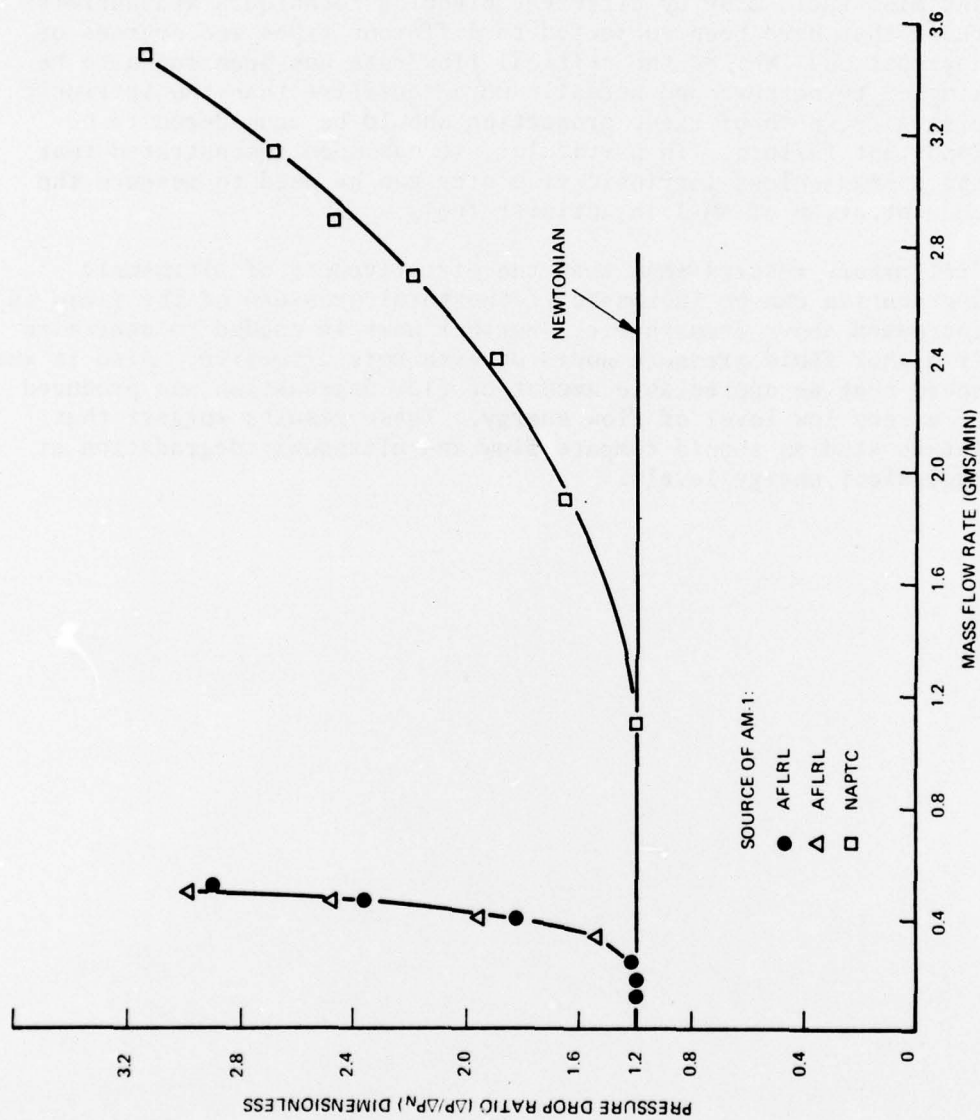


FIGURE 22. ANOMALOUS (VISCOELASTIC) RESISTANCE TO FLOW IN POROUS MEDIA OF ANTIMIST FUELS (0.30% DILUTED TO 0.025% AM-1 in JET-A) USED IN FUEL SPILLAGE/AIR SHEAR TESTS AT NWC.

3. Both the intrinsic viscosity and the critical flow rate in porous media have been shown to be able to distinguish between antimist fuels made with samples of AM-1 obtained from different sources, antimist fuels made by different blending techniques and antimist fuels that have been subjected to different types and degrees of degradation. While, the critical flow rate has been found to be simpler to measure and actually more sensitive than the intrinsic viscosity, both of these properties should be considered to be important factors. In particular, it has been demonstrated that the dimensionless intrinsic viscosity can be used to measure the concentration of AM-1 in antimist fuels.
4. Preliminary results show that the effectiveness of ultrasonic degradation can be increased if the total pressure of the fluid is increased above atmospheric. Further work is needed to determine if higher fluid pressure would be even more effective. Also it was noted that an appreciable amount of flow degradation was produced at a very low level of flow energy. These results suggest that future studies should compare flow and ultrasonic degradation at equivalent energy levels.

LIST OF REFERENCES

1. Billmeyer, F.W., Jr., "Textbook of Polymer Science", 2nd Edition, Wiley-Interscience, New York, 1971.
2. Acierno, D. and Titomanlio, G., "Differences in Behavior Between Dilute and Concentrated Polymer Solutions in Elongational Flow", Chem. Engr. Sci., 29, 1739-1744, (1974).
3. Mannheimer, R.J. and Weatherford, W.D., Jr., "Investigation of Rheological Properties of Dilute Polymer Antimist Agents in Hydrocarbon Fuels", Interim Report AFLRL No. 59 (AD A013502), 1975.
4. Mannheimer, R.J., "The Effect of Solvent and Polymer Properties on the Uncoiling of Flexible Macromolecules in Elongational Flow", In-House Laboratory Independent Research Annual Report (1976).
5. Marshall, R.J. and Metzner, A.B., "Flow of Viscoelastic Liquids Through Porous Media", I&EC Fundamentals, Vol. 6, No. 3, 393-400 (1967).
6. Wright, B.R., et al, "A Technique for Evaluating Fuel Mist Flammability", Interim Report AFLRL No. 25 (AD 776965), 1973.
7. Rouse, P.E., "A Theory of the Linear Viscoelastic Properties of Dilute Solutions of Coiling Polymers", J. Chem. Phys., 21, No. 7, 1272-1280, 1953.
8. James, D.F. and McLaren, D.R., "The Laminar Flow of Dilute Polymer Solution Through Porous Media", J. Fluid. Mech., Vol. 70, Part 4, 733-752 (1952).